

AN ABSTRACT OF THE THESIS OF

MICHAEL JON SCHAER for the Ph. D. in Chemical Engineering
(Name) (Degree) (Major)

Date thesis is presented December 16, 1964

Title A LIQUID SULFUR DIOXIDE BATTERY

Abstract approved 
(Major professor)

A liquid sulfur dioxide battery, such as $K/KCl \cdot SbCl_5$ (0.25 molar) + IBr_3 (15%wt) + SO_2 (l) / carbon matrix is shown to have an open circuit voltage greater than 3.70 volts and an initial voltage of 3.15 volts, decreasing to 2.40 volts in 10 minutes at a current density of 20 ma. /sq. cm. at a temperature of $20^\circ C$. The anode and cathode are in a parallel arrangement and are separated by a distance of 0.15 cm. thus simulating the actual conditions in a wafer type battery. The battery cell is tested at four temperatures in the range $20^\circ C$ to $-44^\circ C$. The performance decreases at the lower temperatures.

The individual types of polarization, such as activation, concentration, and IR drop are isolated. Activation polarization is evaluated for the $Br^0 - Br^-$ cathode and the $Zn^0 - Zn^{++}$ anode by the double pulse galvanostatic method. The rate constant, k_s for the $Br^0 - Br^-$ reaction is evaluated to be 0.23 cm./sec. at $-20^\circ C$. Concentration polarization is mathematically shown to be very small at the current

densities studied (less than 100 millivolts at 20 ma./sq.cm.). The IR drop in the electrolyte contributes appreciably to the total polarization of the cell. However, the largest single factor in the total polarization of the cell is the corrosion film formed on the anode surface by the reaction of the anode with the liquid sulfur dioxide electrolyte. Oxidizing agents, such as water, anhydrous ferric chloride, and anhydrous antimony pentachloride appear to alleviate this polarization somewhat.

Polarization data are tabulated for the dissolution of zinc, magnesium, calcium, lithium, sodium, and potassium. Data are also tabulated for the reduction of IBr_3 on porous stainless steel, flat stainless steel, and a porous carbon matrix.

A LIQUID SULFUR DIOXIDE BATTERY

by

MICHAEL JON SCHAER

A THESIS

submitted to

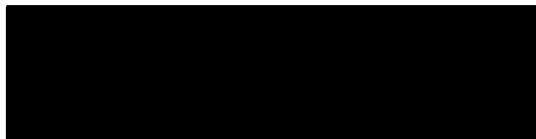
OREGON STATE UNIVERSITY

in partial fulfillment of
the requirements for the
degree of

DOCTOR OF PHILOSOPHY

June 1965

APPROVED:



Associate Professor of Chemical Engineering

In Charge of Major



Head of Department of Chemical Engineering



Dean of Graduate School

Date thesis is presented December 16, 1964

Typed by Lucinda Nyberg

ACKNOWLEDGEMENT

I would like to acknowledge:

The financial support during the course of this work from Oregon State University, the Naval Ordnance Laboratory, Corona, California, and the Texaco Company.

The consultation and advice from Dr. Robert Meredith, Mr. James Divine, Dr. Richard Panzer, and all the staff of the Naval Ordnance Laboratory, Corona.

The assistance on the construction of the experimental apparatus from Mr. Robert Mang and from the Physics Machine Shop.

The typing of the rough draft of this work by my wife, Cara.

TABLE OF CONTENTS

	Page
I. INTRODUCTION	1
Literature Survey	2
Theoretical Treatment of Electrode Polarization.	3
Why a Liquid Sulfur Dioxide Battery	14
II. EXPERIMENTAL APPARATUS	17
Materials	17
Apparatus	17
Polarization Measurements	21
Kinetic Parameter Measurements	21
Conductivity Apparatus	27
Cell Test Fixture and Operating Procedure	28
III. RESULTS AND DISCUSSIONS	32
Reference Electrodes	32
Anodic Polarization of a Zinc Electrode	33
Anodic Polarization of a Magnesium Electrode.	42
Kinetic Parameters of the Bromine-Bromide Cathode Reaction	51
Other Cathode Materials	59
Conductivity of IBr ₃ Solution	59
Battery Cell Tests	60
Introduction	60
Effect of Anode Materials	60
Anode materials in a KCl·SbCl ₅ (0.25 molar) + IBr ₃ (15% wt) + SO ₂ (l) electrolyte	60
Anode material in a FeCl ₃ (sat.) + KBr (sat.) + IBr ₃ (15% wt) + SO ₂ (l) electrolyte	63
Effect of FeCl ₃ and (CH ₃) ₄ NBr on the Cathode Reaction	63
Effect of the Reaction Surface on the Cathode Reaction	67
Effect of the Electrolyte	69
Cathode	69
Anode	69
Current Density Effect	72
Effect of Temperature	74
Summary of Cell Tests	76

	Page
Mathematical Comparisons	77
IV. CONCLUSION	82
BIBLIOGRAPHY	87

LIST OF FIGURES

Figure		Page
1	Polarization of the electrode surface with time	5
2	Polarization versus time.	12
3	Correction for polarization due to diffusion	12
4	Glass polarization cell	19
5	Cell for measurement of kinetic parameters	20
6-A	Electrical circuit for polarization cell (low currents).	22
6-B	Electrical circuit for polarization cell (high currents)	22
7	Overall pulse circuit	24
8	Current pulse power amplifier	25
9	Cell test fixture	29
10	Polarization of zinc anode in liquid sulfur dioxide	35
11	Polarization of zinc anode in liquid sulfur dioxide	36
12	Activation polarization vs. $t_1^{1/2}$	40
13	Magnesium anode polarization	43
14	Magnesium anode polarization	45
15	Magnesium anode polarization	46
16	Magnesium anode polarization	47
17	Magnesium anode polarization	48
18	Magnesium anode polarization	49

Figure		Page
19	$\eta_{\text{Act.}}$ vs. $t_1^{1/2}$ for bromine reaction	55
20	i_o vs. C_{Br^o} for bromine reaction	55
21	Effect of the anode material in the $\text{KCl} \cdot \text{SbCl}_5$ (0.25 molar) + IBr_3 (15% wt) + SO_2 (l) electrolyte at a current density of 20 ma./sq. cm. and at ambient temp.	62
22	Effect of the anode material in the FeCl_3 (sat.) + KBr (sat.) + IBr_3 (15% wt) + SO_2 (l) electrolyte at a current density of 20 ma./sq. cm. and at ambient temperature	64
23	Effect of FeCl_3 and $(\text{CH}_3)_4\text{NBr}$ on the cathode reaction	66
24	Effect of the reaction surface on the cathode reaction. The cell is $\text{Li}/\text{KCl} \cdot \text{SbCl}_5$ (0.25 molar) + IBr_3 (15% wt) + SO_2 (l)/cathode at a current density of 20 ma./sq. cm. and at ambient temperature	68
25	Effect of the electrolyte on the anode	70
26	Current density on the cell $\text{Li}/\text{KCl} \cdot \text{SbCl}_5$ (0.25 molar) + IBr_3 (15% wt)/porous stainless steel at ambient temperature	73
27	Effect of temperature on the cell $\text{Li}/\text{KCl} \cdot \text{SbCl}_5$ (0.25 molar) + IBr_3 (15% wt) + SO_2 (l)/porous stainless steel at 20 ma./sq. cm.	75
28	Mathematical comparison of the cell $\text{Li}/\text{KCl} \cdot \text{SbCl}_5$ (0.25 molar) + IBr_3 (15% wt)/Flat stainless steel plate at a current density of 20 ma./sq. cm. and at ambient temperature	79
29	Comparison of a liquid sulfur dioxide cell and a liquid ammonia cell	85

LIST OF TABLES

TABLE		Page
I	DOUBLE PULSE RESULTS FOR ZINC	40
II	RESULTS OF THE DOUBLE PULSE METHOD FOR BROMINE-BROMIDE REACTION	56

A LIQUID SULFUR DIOXIDE BATTERY

I. INTRODUCTION

By a liquid sulfur dioxide battery we mean a battery which utilizes liquid sulfur dioxide as the solvent or carrier for the electrolyte. The particular battery under study has an active metal anode (alkali or alkaline earth series) and a halogen cathode, therefore giving it one of the highest possible open circuit potentials. Because it does not contain water, it also has the ability to operate at temperatures well below 0° C.

It is the purpose of this work to study not only the final battery cell, but also to develop an understanding of the mechanism of the many aspects of this battery such as the individual anode and cathode reactions, the various types of polarization of these electrodes, and in general, anything which is beneficial to a basic understanding of this battery. It is also the purpose of this work to evaluate electrode reaction kinetic parameters by the double pulse galvanostatic method and to show that the method is feasible in a practical battery electrode reaction.

Literature Survey

Previous work on liquid sulfur dioxide batteries is very sparse. To our knowledge there exists only the work of Schaschl and McDonald (16) in which the possibilities of a liquid sulfur battery are actually explored experimentally. They utilize a magnesium or sodium anode and a cathode composed of iodine, bromine, and ferric chloride, and their best results give an open circuit voltage of 3.5 volts at room temperature and 2.7 volts at -60°C and short circuit current densities of 70 ma./sq. cm. and 16 ma./sq. cm. respectively. The patent by Hajek (11) discusses batteries and accumulators using alkali and alkaline earth metals anodes. However, the patent is rather general and one could only possibly say that liquid sulfur dioxide is included as an electrolyte. Konecny (13) reports on the possibilities of a liquid sulfur dioxide battery but does not discuss any new experimental results.

There are many good reviews of liquid sulfur dioxide chemistry. The two most recent are by Elving and Markowitz (8) in 1960 and Audrieth and Kleinberg (1) in 1953. These reviews have many references to previous work and also correct some of the errors which have been made in the past.

Of particular interest to this thesis are publications which include actual electrochemical reactions. The works of Steele (17),

Bagster and Steele (2), Cady and Taft (5), Bruner and Bekier (4), and Centnerszwer and Drucker (6) discuss electrolysis of salts in liquid sulfur dioxide. An extensive paper by Cruse (7) discusses the behavior of reference electrodes in liquid sulfur dioxide. Finally, two papers by Elving, Markowitz, and Rosenthal (10, 4) discuss voltammetry in liquid sulfur dioxide.

Two papers by Delahay (3, 15) describe the double pulse method used for obtaining the kinetic parameters (exchange current density and transfer coefficient) of an electrode couple. These papers contain the complete mathematical derivations and all the necessary experimental procedures required to apply this method to liquid sulfur dioxide electrolytes. In addition, Laitinen (14) applies this method to the determination of exchange currents in fused salts. The theory of exchange current densities and transfer coefficients is discussed in detail in many general electrochemistry textbooks making it unnecessary to repeat this theory here.

Theoretical Treatment of Electrode Polarization

When an electrode is discharged either spontaneously or by a constant current pulse, a number of polarization phenomena are observed to take place. These can be listed as follows: concentration polarization, activation polarization at the electrode surface, capacitive discharge of the double layer, and resistive polarization

in the electrolyte. These phenomena are described graphically in Figure 1. At time t_0 , the electrode is discharged or pulsed at constant current. Instantaneously the polarization increases to a value equal to the resistive loss between the reference electrode and the electrode under study. Also at time t_0 , the electrode double layer, which is acting as a parallel plate capacitor, starts to discharge. If the rate of electrochemical reaction is fast, the capacitive discharge will tend to obscure the activation polarization. The capacitive discharge is itself very fast, i. e., on the order of 25 microseconds. After 25 microseconds, the increase in polarization is due entirely to concentration polarization caused by the slow diffusion of reactant ions to the electrode surface, diffusion of the products from the electrode, or a combination of both.

Some of the polarizations described in the preceding section can be expressed in a mathematical model where the total polarization is written as the sum of the individual polarization terms, i. e.,

$$\eta_{\text{total}} = \eta_{\text{resistive}} + \eta_{\text{capacitive}} + \eta_{\text{activation}} + \eta_{\text{conc.}} \quad (1)$$

It is observed in Figure 1 that resistive and activation polarization are not functions of time while capacitive discharge and concentration polarization are functions of time.

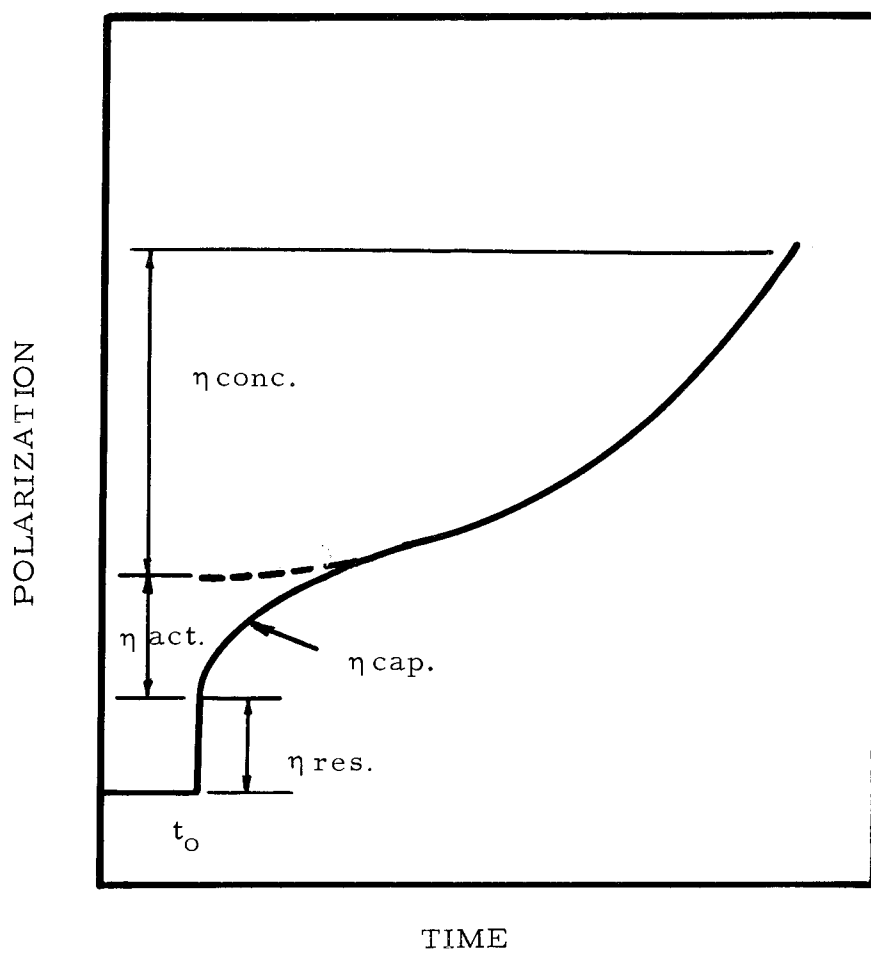
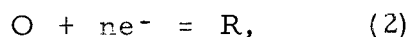


Figure 1. Polarization of the electrode surface with time.

Concentration polarization is dependent upon such things as the geometry of the two electrodes, the total amount of reactant present, the current density, etc. A realistic model would be an actual battery cell made up of two closely spaced parallel electrodes. Let us assume that the electrochemical reaction



where O is the oxidized species and R is the reduced species*, is taking place on one of the electrodes at constant current density. Let us further assume that the species O and R are not affected by the other electrode, that is, the other electrode is a non flux surface to O and R and that there are no end effects. If we assume a negligible electrical migration term and a negligible bulk motion term, then the diffusing species will follow Fick's Law.

Mathematically the diffusion problem can be written as the two differential equations

$$\frac{\partial C_O}{\partial t} = D_O \frac{\partial^2 C_O}{\partial x^2} \quad \text{and} \quad \frac{\partial C_R}{\partial t} = D_R \frac{\partial^2 C_R}{\partial x^2}$$

where C_O and C_R are the concentrations of species O and R, D_O and D_R are the diffusion coefficients of O and R, x is the distance from the no flux surface and t is time. The boundary conditions are

* O and R can be charged species.

$$\left(\frac{\partial C_O}{\partial x} \right)_O = \left(\frac{\partial C_R}{\partial x} \right)_O = 0$$

and

$$D_O \left(\frac{\partial C_O}{\partial x} \right)_L = - D_R \left(\frac{\partial C_R}{\partial x} \right)_L = \frac{i}{n\mathfrak{F}}$$

where L is the distance between the two electrodes, i is the current density, n is the electron change, and \mathfrak{F} is Faraday's constant. The initial conditions are

$$C_O = C_O^0 \quad \text{and} \quad C_R = C_R^0 .$$

The solution of the two differential equations is the same except for nomenclature and sign and hence, only the first solution is given in this work. It is

$$C_O = C_O^0 - \frac{iL}{n\mathfrak{F}D_O} \left[\frac{D_O t}{L^2} + \frac{x^2}{2L^2} - \frac{1}{6} - \frac{2}{\pi^2} \sum_{j=1}^{\infty} \frac{\cos j\pi}{j^2} \cos\left(j\pi \frac{x}{L}\right) \exp - \left(\frac{j^2 \pi^2 D_O t}{L^2} \right) \right] \quad (3)$$

At the electrode surface, $x = L$, it is

$$C_O = C_O^0 - \frac{iL}{n\mathfrak{F}D_O} \left[\frac{D_O t}{L^2} + \frac{1}{3} - \frac{2}{\pi^2} \sum_{j=1}^{\infty} \frac{1}{j^2} \exp - \left(\frac{j^2 \pi^2 D_O t}{L^2} \right) \right] .$$

The potential of the electrode, assuming that concentrations are equivalent to activities, is

$$E = E^{\circ} + \frac{RT}{n\mathcal{F}} \ln \frac{C_{\text{O}}}{C_{\text{R}}} \quad (4)$$

Then at any time after the electrical current starts to flow, the concentration polarization will be

$$\eta_{\text{conc.}} = \frac{RT}{n\mathcal{F}} \ln \frac{1 - iL\omega_{\text{O}}/n\mathcal{F}D_{\text{O}}C_{\text{O}}^{\circ}}{1 + iL\omega_{\text{R}}/n\mathcal{F}D_{\text{R}}C_{\text{R}}^{\circ}} \quad (5)$$

$$\text{where } \omega_{\text{O}} = \frac{D_{\text{O}}t}{L^2} + \frac{1}{3} - \frac{2}{\pi^2} \sum_{j=1}^{\infty} \frac{1}{j^2} \exp - \left(\frac{j^2 \pi^2 D_{\text{O}}t}{L^2} \right)$$

$$\text{and } \omega_{\text{R}} = \frac{D_{\text{R}}t}{L^2} + \frac{1}{3} - \frac{2}{\pi^2} \sum_{j=1}^{\infty} \frac{1}{j^2} \exp - \left(\frac{j^2 \pi^2 D_{\text{R}}t}{L^2} \right)$$

As a point of interest, another form of the solution to the differential equation which is valuable for small time problems since it converges rapidly is

$$C_{\text{O}} = C_{\text{O}}^{\circ} - \frac{2iLQ}{n\mathcal{F}D_{\text{O}}} \sum_{J=0}^{\infty} \text{ierfc} \frac{1+2j-x/L}{2Q} + \text{ierfc} \frac{1+2j+x/L}{2Q} \quad (6)$$

$$\text{where } Q = \frac{D_{\text{O}}^{1/2} t^{1/2}}{L}$$

Activation polarization can be related to the activation energy of the reactive species. Activation energy, itself, is described as an energy which the reactive species must attain in order for it to react electrochemically. In order to attain this energy the potential of the double layer must be offset from the equilibrium potential by some finite value. The electrode current density for the reaction in Equation 2 is shown by Delahay (14) to be a function of the activation polarization and is written as

$$i = i_o \left[\exp \frac{n(1-\alpha)\mathcal{F}\eta_{act.}}{RT} - \exp \frac{n(\alpha-1)\mathcal{F}\eta_{act.}}{RT} \right] \quad (7)$$

where α is the transfer coefficient and i_o is the exchange current density. i_o is defined as

$$i_o = n\mathcal{F} k_s C_O^{(1-\alpha)} C_R^{(\alpha)} \quad (8)$$

where k_s is the reaction rate constant. However, in the case where

$$\frac{n\alpha\mathcal{F}\eta_{act.}}{RT} < 0.02,$$

Equation 7 can be written as

$$\eta_{act.} = \frac{RT}{n\mathcal{F}} \ln \frac{i}{i_o} \quad (9)$$

Capacitive discharge is actually a negative polarization term.

It shows itself in the initial stages of polarization and tends to decay exponentially towards the polarization potential due to concentration.

Resistive polarization can be written as

$$\eta_{\text{resistive}} = IR \quad (10)$$

where R is the resistance between the opposing electrode and the electrode where the reaction is taking place and I is the current.

The preceding mathematical treatment should give one an insight into the polarization of an electrode. However as in all real systems, the simplifying assumptions do not always hold. Examples of irregularities are the formation of a thin film or scale on the electrode surface due to the formation of insoluble reaction products, the dependence of the diffusion coefficient on concentration, and the errors involved when one equates concentration to activity. In some cases the electrode itself can react chemically with the electrolyte solution leading to formation of various products which can affect the electrochemical reaction. Also, the presence of any film will cause an ohmic polarization due to the high resistance of such a film. Therefore, in all electrode reactions, one should be extremely careful in the interpretation of the observed results for such results may be influenced by the irregularities described above.

As mentioned before, a fast electrochemical reaction will be obscured by capacitive discharge. To alleviate this problem,

Delahay (15) discusses the double pulse galvanostatic method for fast electrode reactions. This is discussed in brief in the next paragraph.

The double pulse method consists of pulsing the electrode with two constant-current pulses where the first pulse is of a greater magnitude than the second pulse. The first pulse of length t_1 has the lone requirement of quickly (< 10 microseconds) discharging the capacitive charge of the electrode double layer so that the polarization of the electrode at that time is exactly equal to the activation polarization plus any concentration polarization up to that time. The second current pulse then continues from t_1 causing continued polarization which varies only with the concentration polarization and is not dependent upon the capacitive discharge. Figure 2 shows the work of Delahay (15) where the electrode was pulsed at various i_1/i_2 ratios. The curve with a horizontal tangent at t_1 is also shown by Delahay to give the correct value of the activation polarization plus the concentration polarization at time t_1 . The polarizations are recorded at several values of t_1 and these values are then plotted against $t_1^{1/2}$ and extrapolated back to where $t_1^{1/2}$ is equal to zero as shown in Figure 3. The value of η at $t_1^{1/2}$ equal to zero, is exactly equal to the activation polarization at the current density of the second pulse and does not include any concentration polarization.

Delahay's double pulse method also allows one to obtain the diffusion coefficients of the reacting species from the slope of the plot of

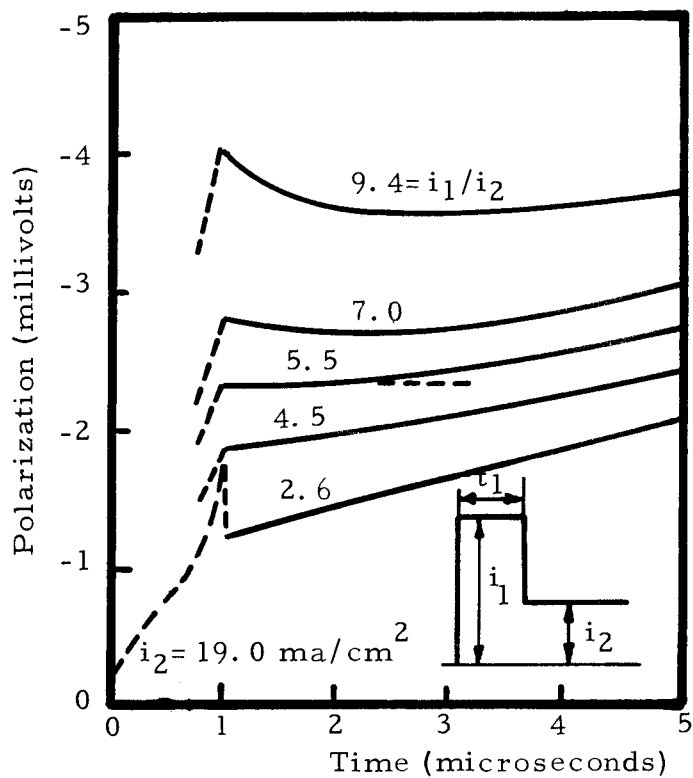


Figure 2. Polarization versus time.

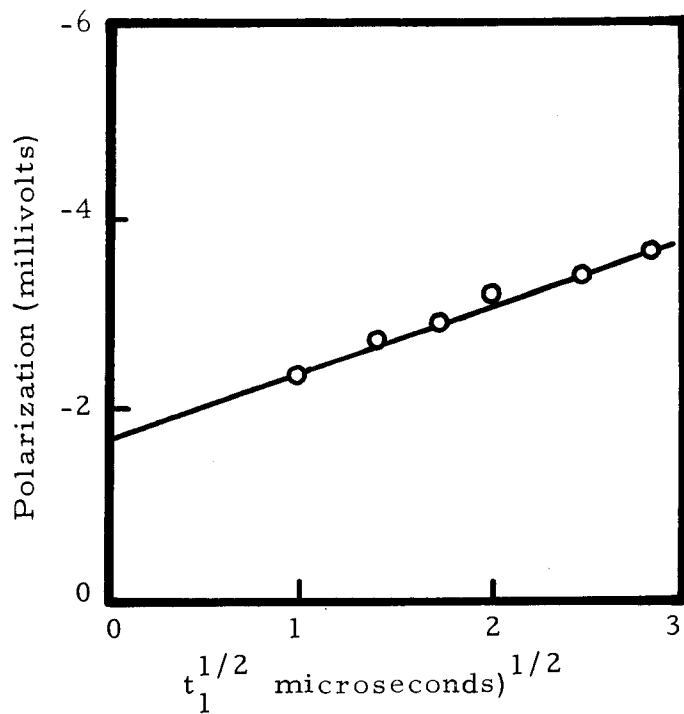


Figure 3. Correction for polarization due to diffusion.

polarization vs. $t_1^{1/2}$. One must however, remember that a theoretical model can only be extended so far before it starts to break down. In cases where some of the assumptions are on the marginal side, the calculation of diffusion coefficient from this slope may lead to erroneous results.

It is important to determine the value of the exchange current, for if this value is small it will indicate that the electrode will be kinetically unfavorable as an electrode in a high energy battery system. If the electrode has an exchange current of less than 0.1 ma./sq. cm. it will have an activation polarization (charge transfer) of 0.1 volts at 10 ma./sq. cm. However, if the electrode has an exchange current greater than 100 ma./sq. cm. it will theoretically have an activation polarization of 0.1 volt at 10 amps/sq. cm.

All real batteries will contain some concentration and resistive polarization. In many batteries one is powerless to do anything about decreasing them. The resistive polarization is determined entirely by the conductivity of the electrolyte. Once an electrolyte has been selected, this polarization is fixed and cannot be decreased. Concentration polarization is a direct function of the diffusion coefficients and the cell geometry. Most substances have a diffusion coefficient in the neighborhood of 10^{-5} sq. cm./sec. and hence this puts a limit on the amount of reduction in polarization that one can obtain from changing the reactive species.

In many cases, if one had only activation, resistive, and concentration polarization to be concerned with, problems would be very few indeed. However, one primary problem in battery polarization is the mechanical formation of obstructive films next to the electrode. These films decrease the active sites of possible electrochemical reaction and hinder the mass transport of conducting ions to these active sites. To date, the theoretical treatment of polarizing films as applied to batteries has been limited.

In summary, one must remember that any theoretical treatment is always a step forward, but one should take care when applying any completely theoretical equation to a real system. At any time, especially in the case of high energy batteries, other factors may totally obscure the factors which have been treated theoretically.

Why a Liquid Sulfur Dioxide Battery

A liquid sulfur dioxide battery can operate over a wide temperature range. Sulfur dioxide is in a liquid form at temperatures below -50° C and will remain liquid at room temperatures and higher when under pressure. Such an efficient low temperature battery is necessary in an application where there is a wide temperature variance, such as, in a military application in the arctic regions. Such a battery could also be used in a space probe that was shielded

from the sun.

A liquid sulfur dioxide battery can be constructed so that the liquid electrolyte is enclosed in a container separate from the electrode compartment. At the time of activation, the electrolyte is injected into the electrode compartment. This would allow such a battery to be stored indefinitely without any deterioration taking place.

Since some liquid sulfur dioxide solutions are compatible with the alkali metals, one could obtain a much higher overall potential per cell and therefore reduce the total number of cells required for a battery of a particular voltage.

Liquid sulfur dioxide is relatively easy to handle, and, although somewhat toxic, it cannot be considered among the very toxic gases such as hydrogen sulfide, etc. Also, liquid sulfur dioxide is relatively cheap and is readily available in anhydrous high purity grade.

There has been and still is a need for a high energy, short life (under one hour) battery. In the past, fused salt batteries have been used to fill this requirement, but their life times have been too short. As the need develops, batteries with nonaqueous solvents are being tested and developed. Liquid ammonia has been very successful in filling some of the present requirements. However, there is no

reason to believe that any one nonaqueous solvent is the best solvent for every type of battery. Therefore this thesis investigates the feasibility of a battery utilizing liquid sulfur dioxide electrolytes.

II. EXPERIMENTAL APPARATUS

Materials

The sulfur dioxide gas is the anhydrous grade purchased from the Matheson Company. It is further purified by passing it through concentrated sulfuric acid to remove any sulfur trioxide present and then across phosphorus pentoxide to remove any residual water. It is finally introduced into the apparatus and condensed.

The chemicals which are used are all dried in a vacuum oven and then transferred into a dry box where they remain. Most of the chemicals are of the highest purity possible but in some cases, where a high degree of accuracy is not required, the poorer grades are substituted.

Apparatus

The cold bath is made by connecting a war surplus compressor (approximately one ton capacity) to an Aminco temperature bath (Model 4-86E). The circulating fluid is a mixture of ethyl alcohol and water with its temperature maintained to $\pm 0.5^{\circ}$ C with an Aminco "Quickset" bimetal thermoregulator. With this apparatus, temperatures as low as -50° C and temperatures as high as 25° C can be obtained. Higher temperatures increase the vapor pressure of the alcohol and causes a loss due to evaporation. The temperature is

measured by measuring the resistance of a Fenwal LB21J1 thermistor (using an Eico decade resistance box, Model 1171) which has been calibrated against a platinum resistance thermometer. The platinum resistance thermometer has in turn been calibrated by the National Bureau of Standards.

The polarization cell (Figure 4) consists of a two compartment U-tube separated by a medium fritted glass disc. Each section of the tube has a volume of approximately 35 ml. The electrodes are sealed in the cell by means of standard taper glass joints. One compartment contains the electrode of interest along with a reference electrode inside a small glass tube shaped like a Luggin capillary, and the other compartment contains only a working electrode.

The apparatus (Figure 5) which is used for the measurement of the kinetic parameters is a three necked flask with standard taper joints. The indicator electrode, a platinum wire (0.010 inch dia.) which is sealed in a glass tube and ground flush to the tube surface, is inserted through the left opening. The working electrode is a large metal electrode (greater than 5 sq. cm.) and is inserted through the right opening. The middle opening is used for filling the flask with sulfur dioxide.

A dry box was constructed in order to handle all hygroscopic materials and also all of the active anode materials. It is of the circulatory type with the gas moving through a molecular-sieve bed to remove water and through a copper-shaving bed (500° C) to remove

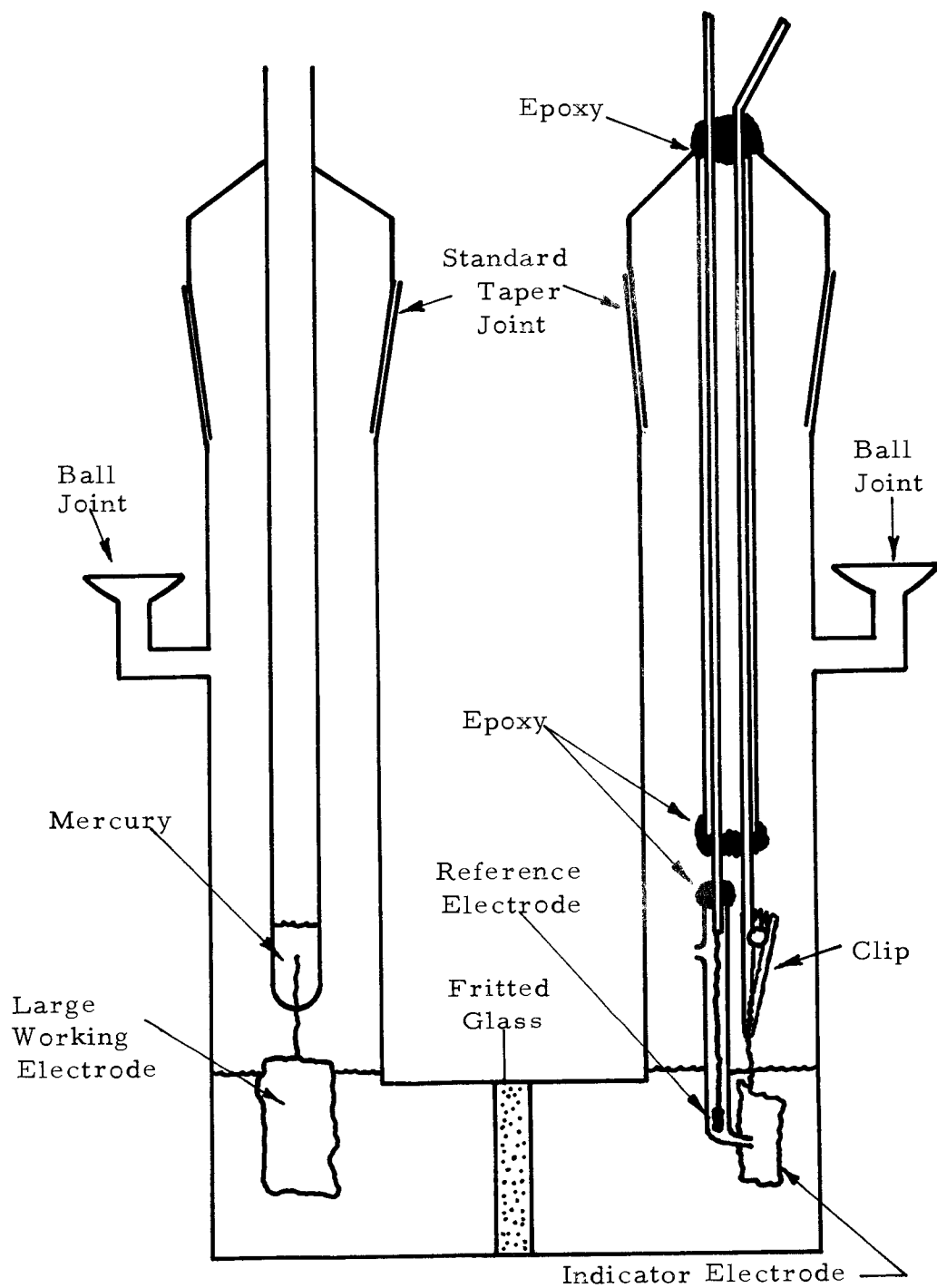


Figure 4. Glass polarization cell.

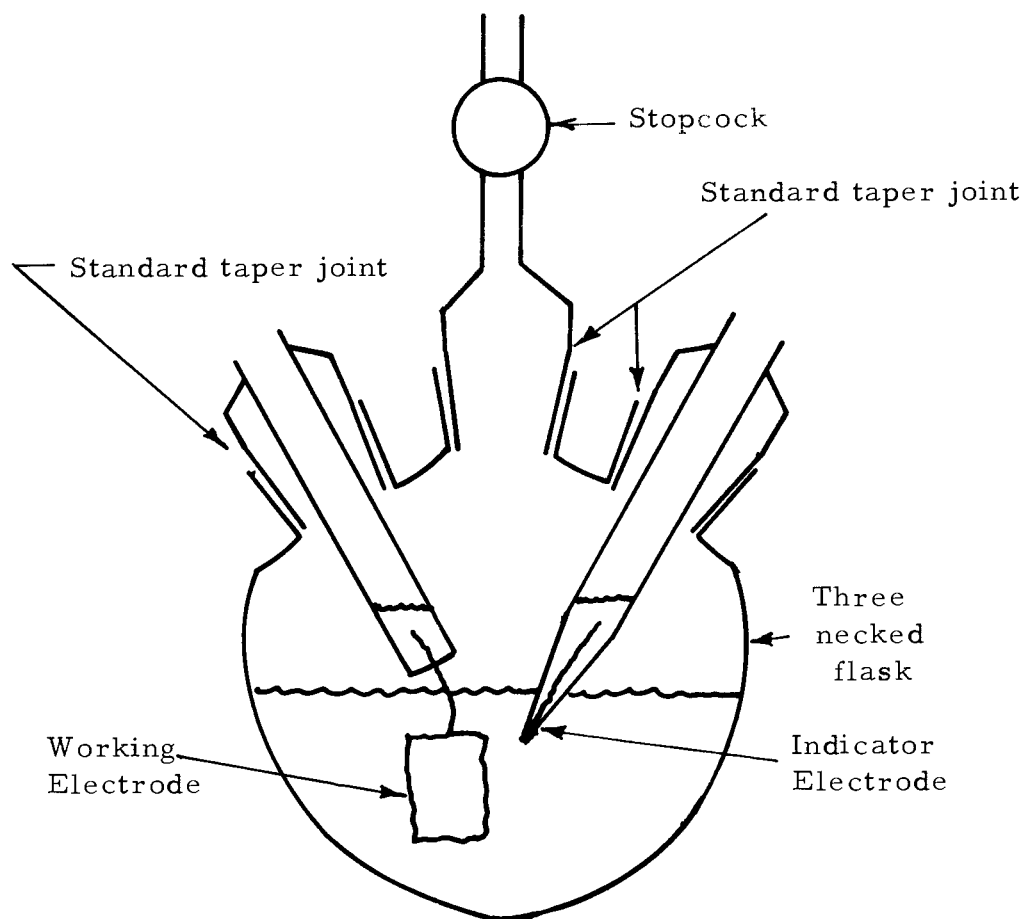


Figure 5. Cell for measurement of kinetic parameters.

oxygen. The molecular sieve is regenerated by heating (500° C) and passing dry nitrogen through it. The copper shavings are regenerated by passing hydrogen through them.

Polarization Measurements

The electrical circuit diagram for the polarization cell shown in Figure 4 is shown in Figure 6-A. The purpose of the high voltage source and the variable resistor is to maintain the current through the circuit at a constant value. This will occur if the voltage drop across the variable resistor is much greater than the voltage drop across the cell. In Figure 6-B a constant current source (Power Designs Inc. , Model TW -4005) is substituted for the high voltage source and variable resistor. The constant current source was limited to the range of 25 ma. to 1000 ma. , otherwise it would have been used throughout all of the polarization runs.

The current is measured with either a calibrated milliammeter or a micro-microammeter (Keithley Model 411). The potential is measured on a strip chart recorder (Varian G-11A) and, in order to verify the readings, a vacuum tube voltmeter (Knight) is also used. All instruments are calibrated against a potentiometer (Leeds and Northrup Model K-2) with a standard cell traceable to the Bureau of Standards.

Kinetic Parameter Measurements

The electrical circuits for the measurements of the kinetic

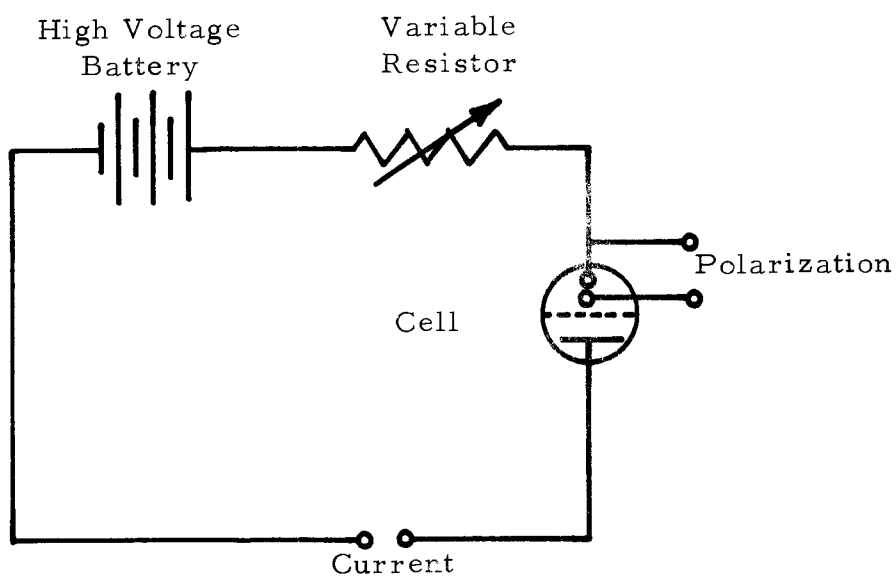


Figure 6-A Electrical circuit for polarization cell (low currents).

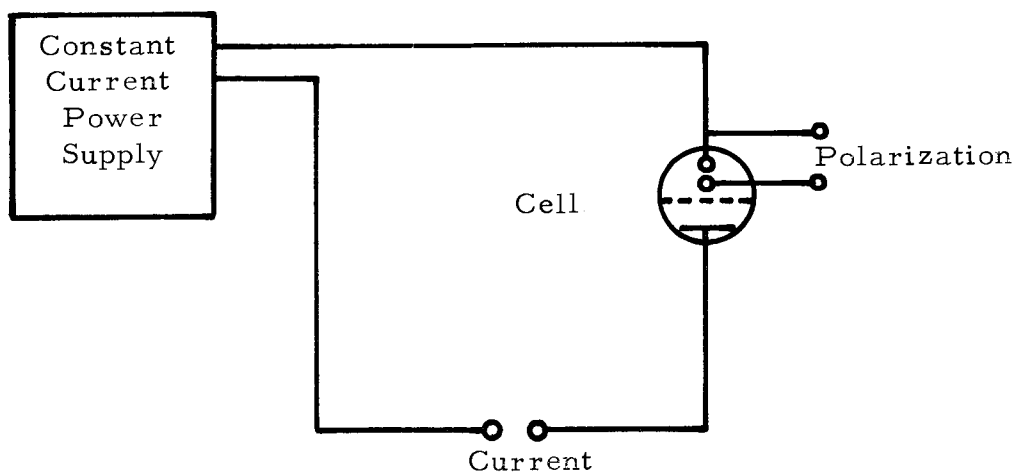


Figure 6-B. Electrical circuit for polarization cell (high currents)

parameter, i_o , are shown in Figures 7 and 8. Figure 7 shows the overall experimental apparatus. The waveform generator (Tektronix 162) activates the two voltage pulse generators (Tektronix 163). These voltage pulses are then converted into current pulses by the power amplifier shown in Figure 8 (discussed in the next paragraph). The polarization across the cell is amplified (Tektronix 1121) and displayed on the oscilloscope (Tektronix 545A with a type CA preamp) with the trace triggered by the waveform generator. The current is also measured on the oscilloscope by recording the potential drop across the fixed resistor, R_2 , since the same current flows through each leg of the bridge type circuit in the power amplifier. (Note: current measured on independent run). The waveform generator and both pulse generators are powered by an external supply (Tektronix 160A).

The power amplifier shown in Figure 8 is similar to the one designed by Delahay (15) with some modifications. The amplifier can be broken down into several components: the amplifier section, the bridge circuit section, the zero-current balance section, and the bias section. The amplifier section is composed of tubes T_1 and T_2 (both 6J6A), battery B_1 (45 to 200 volt battery), and two grid resistors R_3 and R_4 (each 200 ohms). R_3 and R_4 must be kept low in order to increase the rise time of the circuit. The bridge circuit section is composed of resistors R_1 and R_2 (each 216 ohms (must be identical)), resistor R_6 (50 ohm adjustable),

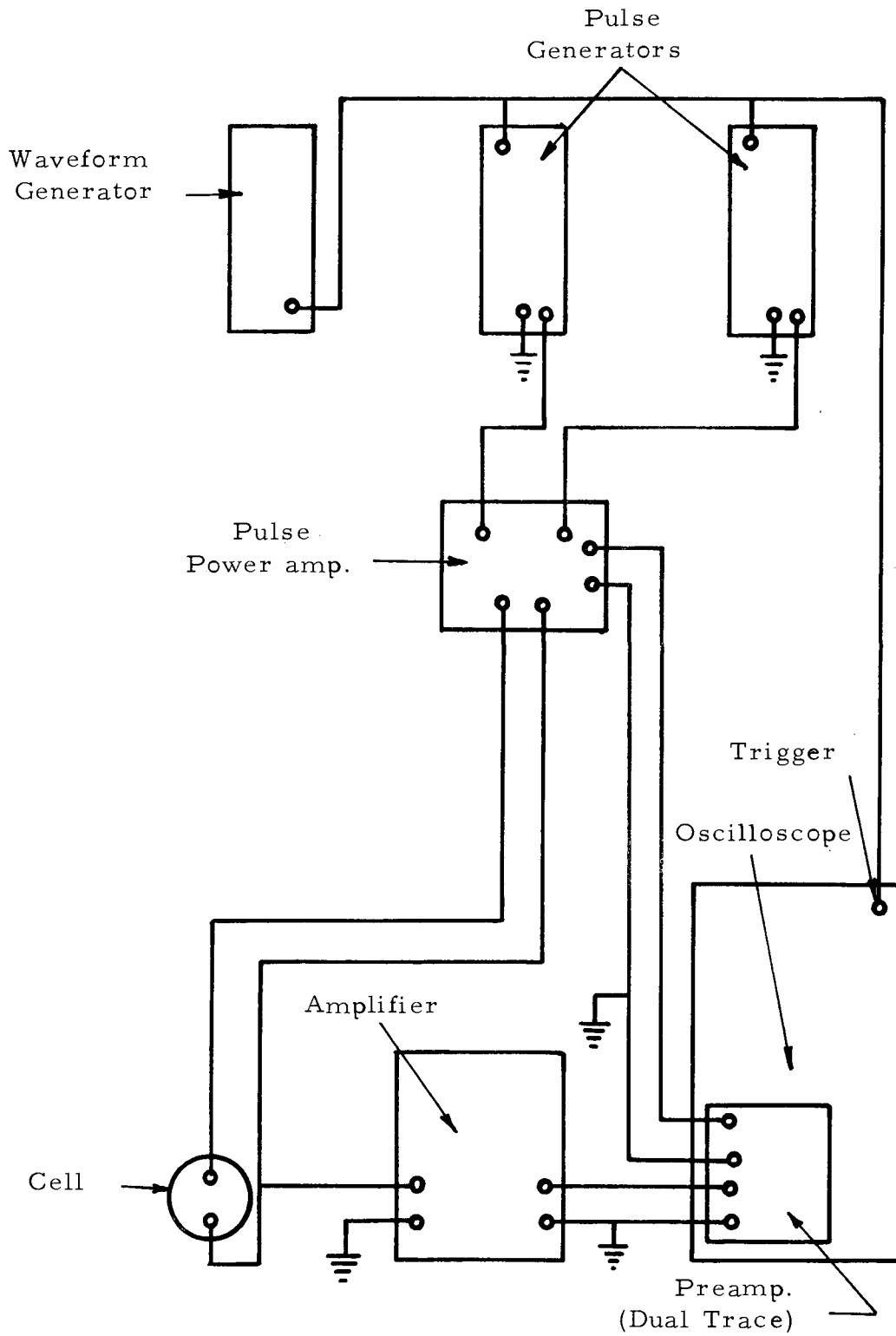


Figure 7. Overall pulse circuit.

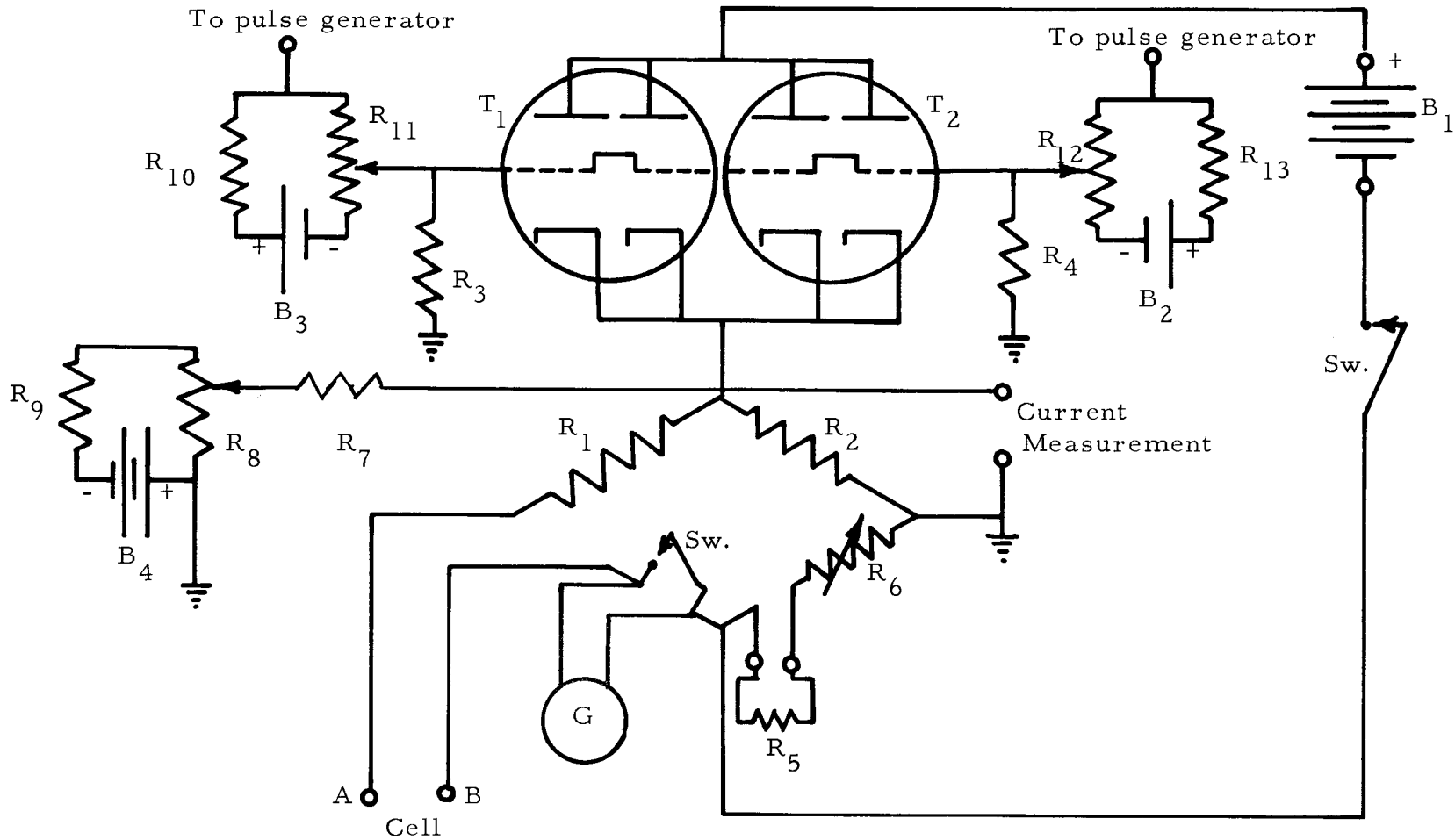


Figure 8. Current pulse power amplifier.

and resistor R_5 (value depends upon the type of electrolyte in the cell). This section allows the cell solution resistance to be subtracted from the polarization measurements. Note that if the cell has zero polarization at the electrode surface, then the potential measured from A to ground will be zero, and therefore, only the polarization at the electrode surface will be observed. The zero current balance section is composed of resistors R_7 , R_8 , and R_9 (5000 ohm, 1000 ohm adjustable, and 2000 ohm respectively), battery B_3 (45 volts), and a galvanometer, G. The purpose of this section is to cancel out the residual current of the tubes when there is no voltage pulse. Both grid bias sections are identical and are composed of resistors R_{10} and R_{12} (500 ohm each), resistors R_{11} and R_{12} (200 ohm adjustable each), and batteries B_2 and B_3 (22.5 volt each). This section provides a negative bias to the tubes in order to reduce the residual current to a very small value, and it also allows the adjustment of the current pulses. It is important that batteries B_2 and B_3 are of low internal resistance in order to increase the rise time of the circuit.

It is interesting to note that the possibility of saturation of the oscilloscope amplifier is greatly reduced by placing the ground between resistors R_2 and R_6 , because only the change in actual polarization of the electrode surface is amplified. Saturation of an amplifier takes place when the input voltage exceeds the designed voltage range of the amplifier. In Delahay's (15) circuit, this is possible if the

electrolyte resistance is large since he uses two amplifiers in a differential measuring circuit. The first amplifier records the electrolyte voltage drop and the second amplifier records the electrolyte voltage drop plus the activation and concentration polarization. The two outputs are then subtracted from one another electronically to give only the activation and concentration polarization. However, one must remember that both amplifiers are amplifying the voltage drop across the electrolyte and a high voltage drop will cause saturation of both amplifiers. In our circuit the potential drop across the electrolyte is not amplified and hence the saturation problem in Delahay's circuit is avoided.

Conductivity Apparatus

The conductivity is measured in a glass U-tube containing two platinum-black electrodes with a cell constant of 36.1 cm.^{-1} . The vessel is completely sealed from the atmosphere and the liquid sulfur dioxide is injected from a completely sealed volumetric flask. The liquid electrolyte is forced into the conductivity cell by means of applying a dry nitrogen gas pressure to the sealed volumetric flask. The entire apparatus is immersed in the cold bath in order to avoid boiling in the connecting lines. The resistance of the solution is measured with an Industrial Instrument Type RC Conductivity Bridge at 1000 cycles/second.

Cell Test Fixture and Operating Procedure

The apparatus (Figure 9) which is used for the testing of actual complete cells is machined from stainless steel. The connecting tubing is stainless steel and the valves are also stainless steel with Teflon seals. The gaskets on the cell test fixture as well as on the electrolyte container are fabricated from Neoprene. All the gasket materials tried are attacked by the electrolyte solution with the exception of Teflon.* The Neoprene gaskets are attacked and hence they have to be replaced when they became ineffective. Teflon did not work as a gasket material because it does not contain the soft compressible properties necessary for a vacuum tight seal. Also, the stainless steel is attacked somewhat by the electrolyte solution but this effect is very small.

The electrochemical cell to be tested is located in the center of the cell test fixture. It consists of a porous, stainless steel disc (1/32-inch Bendix Corporation Poroplate) which makes contact with the upper stainless steel section of the fixture through a stainless steel disc and a steel spring. The anode material is pressed to the bottom stainless steel section, making sure that none of the bottom section is exposed to the electrolyte solution. The anode and the cathode are

*At a later date, polyethylene was tested and found to be unattacked by the electrolyte solution.

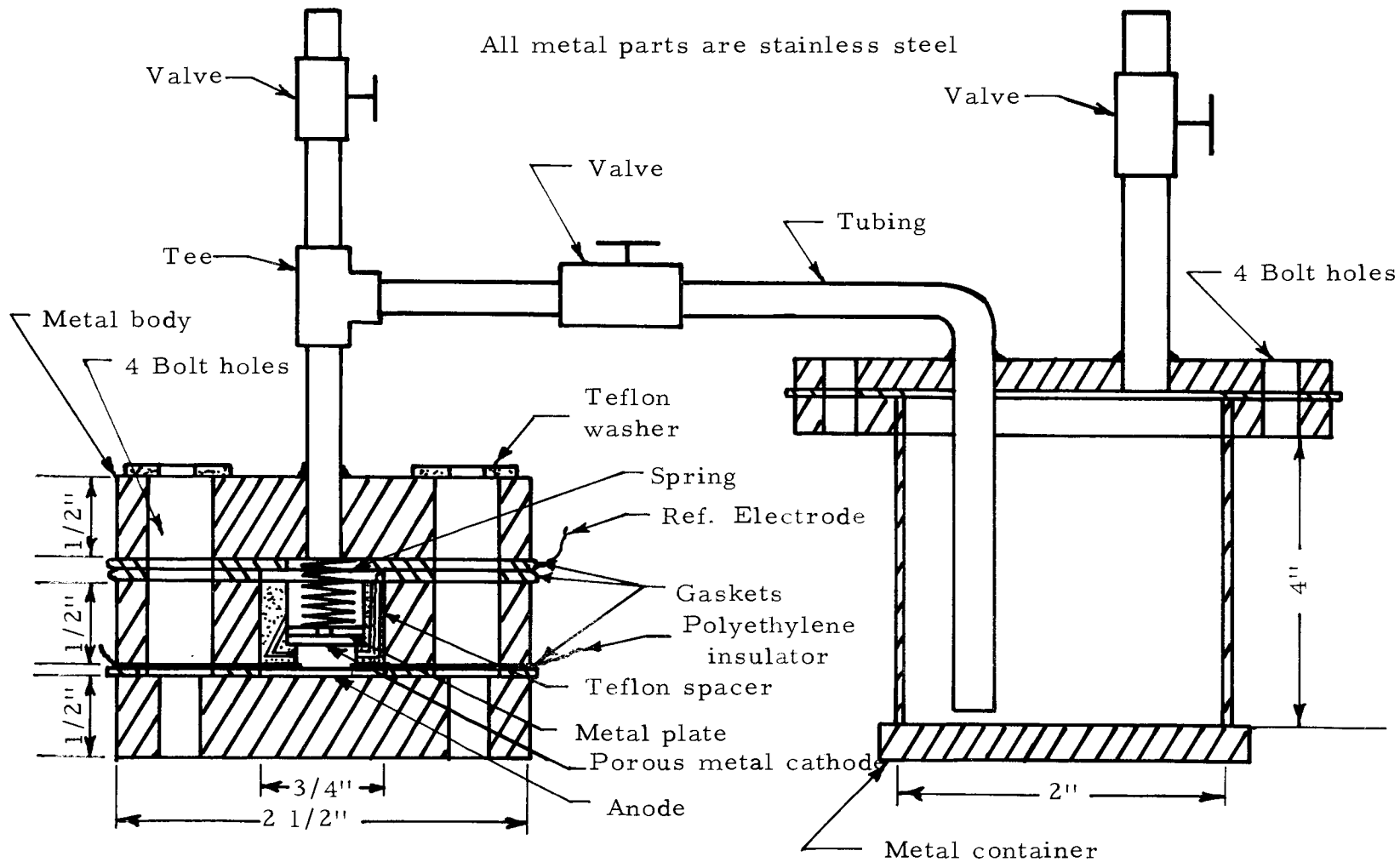


Figure 9. Cell test fixture.

separated from each other by the shoulder of the Teflon spacer which supports the cathode disc. There is approximately 0.15 cm. between the anode and the cathode. The whole area of both the cathode and anode is one sq. cm. The reference electrode is a silver wire covered with Teflon tape which has been heated so that it is sealed to the silver surface. Hence the only part of the reference electrode which is in contact with the electrolyte solution is the short end section. The reference electrode is led out between two neoprene gaskets. The center stainless steel section is completely insulated from both ends and serves only as a separator.

The container is a stainless steel tube built to withstand pressures in excess of 200 lbs./sq. in. The inlet and outlet tubing is arranged so that the liquid electrolyte will pass up through the lower tube and into the cell test fixture.

A typical cell test is described directly below. The proper chemicals are added to the container, and then gaseous sulfur dioxide is distilled into the cool container (-20° C) through the top valve. At this time the connecting valve is closed. During this process the air is removed from the container by periodically drawing a slight vacuum on the partially condensed liquid sulfur dioxide. When a proper amount of sulfur dioxide is added (determined by difference weighing), the valve is closed and the container is removed from the cold bath and allowed to come to room temperature.

At room temperature the internal pressure is about 50 lbs./sq. in. The container is now ready to supply electrolyte to many individual cell tests.

The anode and cathode materials are arranged inside the cell test fixture while the entire cell test fixture is inside of the dry box. The cell test fixture is then removed from the dry box and connected to the container. The cell is immediately evacuated to less than 100 microns pressure by connecting the vacuum hose to the top valve on the fixture. This valve is then closed and the electrical measuring leads are connected to the reference electrode wire, the top section (cathode), and the bottom section (anode). The electrolyte container is now pressurized with dry nitrogen to about 90 lbs./sq. in. gage. The cell test begins when the connecting valve is opened.

A constant current is obtained in the same way as described in a preceding section on the glass polarization cells. The reference-anode and reference-cathode potentials are recorded on a Texas Instruments dual channel Servo-riter strip chart recorder.

After the test, the connecting valve is closed and the valve on the top of the fixture is opened slowly in a hood and the pressurized electrolyte is allowed to evaporate. The complete cell test fixture is then cleaned before corrosion due to the moisture in the air sets in.

III. RESULTS AND DISCUSSIONS

Reference Electrodes

The silver-silver iodide electrode is prepared according to the procedure outlined by Taniguchi and Janz (18) with the exception of the substitution of potassium iodide for potassium chloride in the electrolysis process. This electrode appears to be stable in the electrolyte of potassium iodide and liquid sulfur dioxide, that is, it retains the potential of 0.080 ± 0.010 volts versus zinc over a period of 24 hours. The electrode, however, has the disadvantage of a high internal resistance, thus requiring the use of high impedance instruments for potential measurements.

During the course of the early experimental work it became apparent that a plain silver wire would serve the purpose of a reference electrode. Consequently, in all the battery cell tests, the reference electrode is an untreated silver wire. In sulfur dioxide solutions which contain bromine or iodine, the impedance of the silver electrode is considerably reduced. The potential of the electrode couple IBr_3 on stainless steel/Ag is consistently between +0.80 volts and +0.95 volts at ambient temperatures. In an aqueous solution at 25°C the potential of the electrode couple $\text{Br}_2/\text{AgBr}/\text{Ag}$ is +0.99 volts. An accurate comparison between these two couples is not possible since they are in different media, but one would expect that they would

be relatively close to one another. The fact that they are close to one another tends to show the practicality of the untreated silver wire reference electrode.

A lead electrode also deserves mention as a possible reference electrode since it retains a steady potential of -0.095 volts vs. the Ag/AgI electrode in a sulfur dioxide solution containing ammonium thiocyanate. Even after a heavy current is applied, the lead electrode still returns to the original potential.

Anodic Polarization of a Zinc Electrode

The polarization of the zinc anode is experimentally determined in the two compartment cell shown in Figure 4. The cathode compartment contains a large platinum electrode (12 sq. cm.) while the anode compartment contains the zinc anode (2 sq. cm.) as well as a glass Luggin capillary tube which encloses a silver-silver iodide reference electrode. Previous to each run the zinc anode is cleaned with a concentrated hydrochloric acid solution which leaves the surface very bright and smooth. The electrolyte is a liquid sulfur dioxide solution saturated with potassium iodide and maintained at a temperature of -20° C. All the salts are extensively dried before each experiment by heating them in vacuo.

The experimental procedure consists of passing a constant current between the platinum and zinc electrode as shown in Figure 6-A

and Figure 6-B and measuring the change of potential between the zinc electrode and the silver-silver iodide reference electrode. Figure 10 shows the polarization over the entire range of current densities and Figure 11 shows the polarization at very small current densities.

The polarization is primarily due to concentration and ohmic effects. The concentration polarization is caused by the build up of zinc ions near the surface. In other words, the solution next to the surface becomes concentrated in zinc iodide thereby making the potential more positive. Once this solution is saturated in zinc iodide, crystals start to form. This reduces the electrochemical reaction surface and thereby increases the polarization. Figure 10 indicates that up to current densities of approximately 3 ma./sq. cm. the electrode can still dissipate the zinc ions into the bulk of the solution. However over 3 ma./sq. cm., the zinc iodide crystals start to cover part of the surface. This is definitely apparent above a current density of 6 ma./sq. cm. where the polarization increases without bound indicating total surface coverage. When the solution is stirred, the polarization is reduced to +0.33 volts at a current density of 11.0 ma./sq. cm. This further verifies the fact that polarization is caused by a build up of zinc iodide on the surface. From the fact that no elemental iodine is formed at the surface at high polarization as in the case of a platinum anode, one concludes

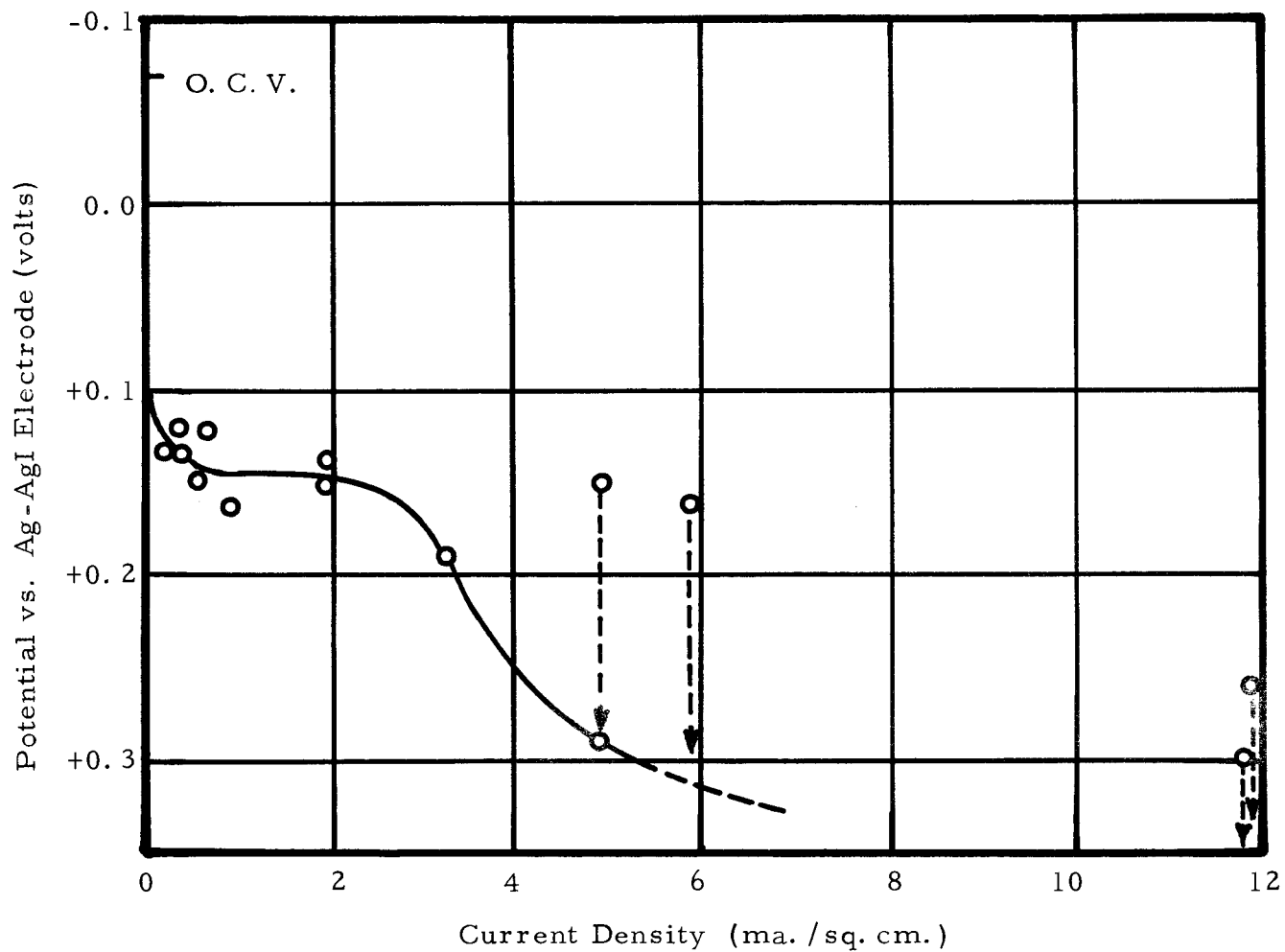


Figure 10. Polarization of zinc anode in liquid sulfur dioxide.

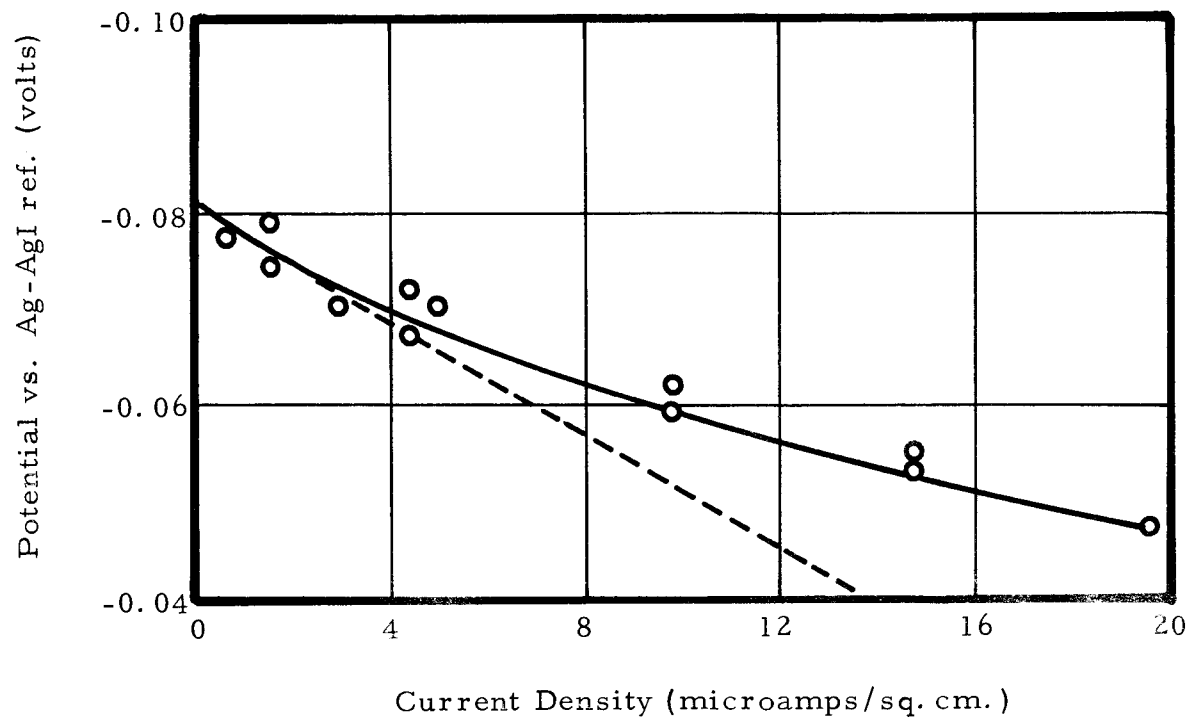


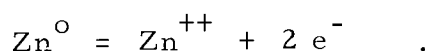
Figure 11. Polarization of zinc anode in liquid sulfur dioxide.

that the potential at the surface is still more negative than the iodine-iodide reaction. Therefore part of the high polarization must be caused by ohmic polarization through the zinc iodide crystals. Finally, visual observation at high current densities (over 10 ma./sq. cm.) indicates that a white solid forms at the surface. This solid must be zinc iodide crystals.

The polarization at small current density can be used to obtain the value of exchange current density (i_o) if the effects of concentration and ohmic polarization are negligible in comparison to the activation polarization (charge transfer). The procedure is to start with Equation 9. This equation can be rewritten as

$$i_o = \frac{RT}{n\mathcal{A}} \frac{i}{(E-E^o)}$$

where i is the current density, i_o is the exchange current density, E is the potential at current density i , E^o is the equilibrium potential, and n is the electron change. The derivation of this equation includes the assumption that $(E-E^o)$ must be less than a few millivolts. The slope of a plot of $(E-E^o)$ versus i will be equal to $-i_o n\mathcal{A}/RT$ provided this is the limiting slope as the current approaches zero. From this slope one calculates the value of i_o to be 3.80×10^{-6} amps/sq. cm. for the reaction

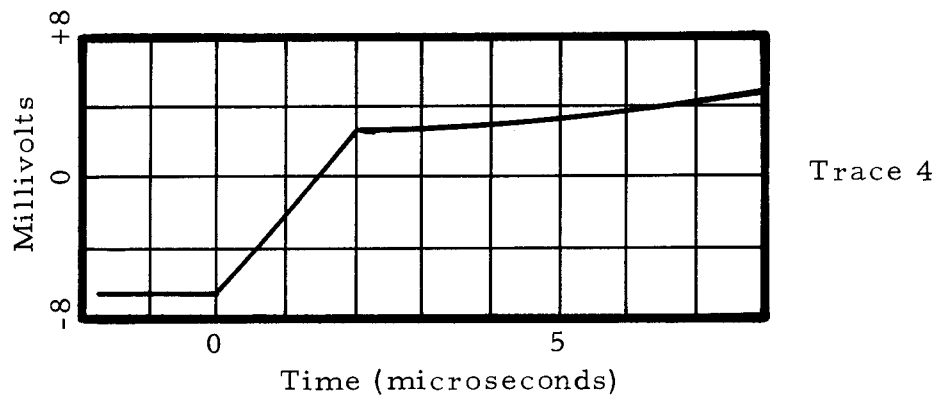
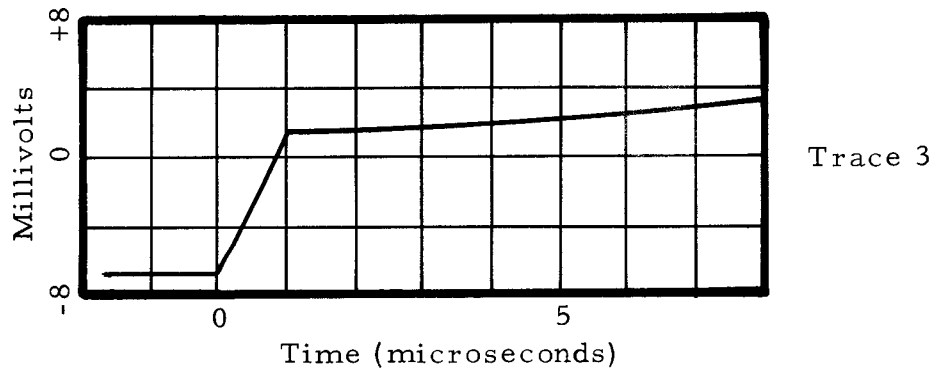
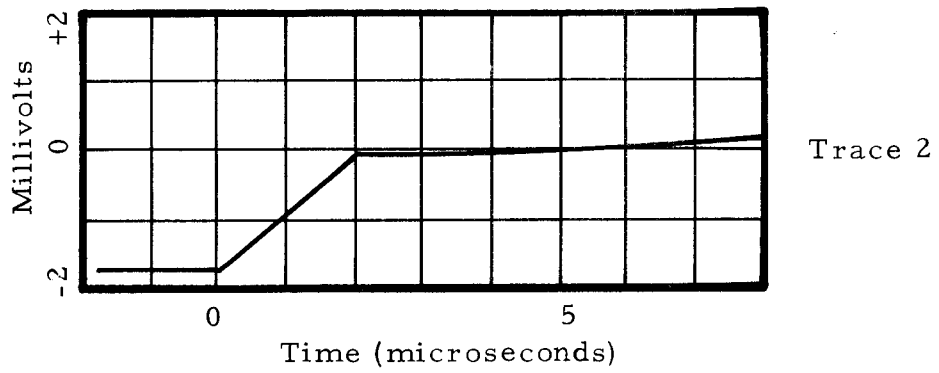
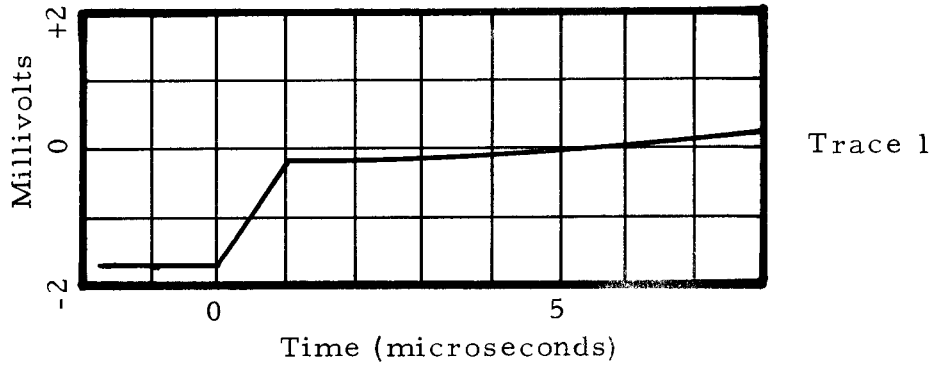


In this calculation n is equal to two and the temperature is 253° K.

The low solubility of zinc iodide gives rise to questions about the assumption of zero concentration polarization at low current densities. The solubility of zinc iodide as tabulated by Audrieth and Kleinberg (5) is 3.45 millimoles/1000 grams of sulfur dioxide or about 1.60 grams/liter at -10° C. If the assumption is incorrect, the value obtained for the exchange current would have been too small.

Possibly a better method for obtaining the exchange current density is the double pulse method since this method avoids the problem of concentration polarization. The cell consists of a three necked flask as shown in Figure 5. It contains a small zinc indicator electrode (anode), and a large zinc working electrode (cathode) of about 6 sq. cm. The electrolyte is a saturated solution of potassium iodide maintained at -20° C. The indicator electrode has an area of 0.000506 sq. cm. and has a layer of zinc plated onto the smooth platinum surface. The zinc plating procedure is obtained from the 1964 Plating Handbook. Examination under a ten power microscope indicates that the surface is not perfectly smooth but is somewhat lumpy in appearance.

The results of the double pulse experiments are shown in Traces #1 through #4 and Table I. The four traces are copied from the original photographs obtained during the experiments and are smoothed to remove the noise picked up from the electronic apparatus. Also



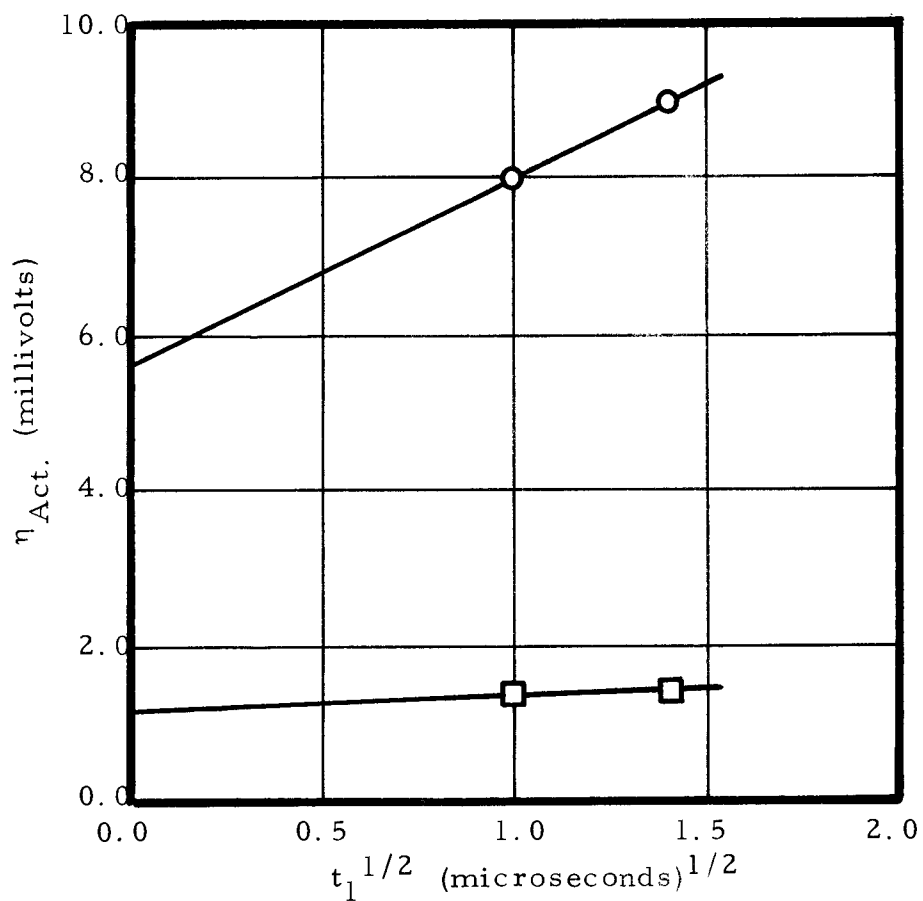


Figure 12. Activation polarization vs. $t_1^{1/2}$.

TABLE I. DOUBLE PULSE RESULTS FOR ZINC.

t_1 microsec.	Current microamp.	$\eta_{act.}$ millivolt	$\eta_{act.}^{t_1 \rightarrow 0}$ millivolt	i_o ma. /sq. cm.
1.0	7.88	1.40		
2.0	7.88	1.45	1.28	132
1.0	44.5	8.00		
2.0	44.5	9.00	5.61	170

Note: i_o calculated from Equation 9.

it is not uncommon to observe some small oscillations on some of the photographic traces. The activation polarization obtained from each of the traces is then plotted against $t_1^{1/2}$ (length of the first pulse) and extrapolated to $t_1^{1/2}$ equal to zero. This process is illustrated in Figure 12. From this extrapolated value of activation polarization, one obtains the exchange current density (i_0) by using Equation 9.

In this case, the exchange current density is between 132 and 170 ma./sq. cm. Therefore the zinc electrode has the kinetic potential of being an excellent anode. However we see that due to the concentration and ohmic polarization at the surface, it fails as a high energy battery electrode. Also the low open circuit potential eliminates zinc as a practical battery electrode.

Also of importance in this section is the fact that the exchange current obtained by the continuous passage of current discussed earlier leads us to an incorrect value of the exchange current density because of the concentration and ohmic polarization. This fact then illustrates the value of the double pulse method.

It should be stated as a final note that the zinc electrode was studied because of its well defined behavior and ease of preparation and at no time was zinc ever considered as an anode in an actual liquid sulfur dioxide battery.

Anodic Polarization of a Magnesium Electrode

Magnesium metal in contact with a 2 molar potassium iodide solution acts as if it is extremely passivated. This passivity can be explained by the presence of a film on the surface. Visual observation indicates that the film is very thin since the metal still retains its original bright appearance when immersed in the electrolyte solution over a period of several hours. The open circuit voltage versus the Ag/AgI electrode is -0.36 volts. Since the Mg/Mg⁺⁺ couple should be much more negative, it must be assumed that the actual electrode couple involved is some other magnesium compound, such as, MgS₂O₅, MgS₂O₃, etc. These compounds can be formed by the reaction of metallic magnesium with the solvent. It can then be concluded that in order to be able to use a highly negative metal as an anode, one must add a compound to the electrolyte which will stop the film formation or a compound which will continuously remove the anodic film.

Figure 13 shows the polarization of the magnesium anode in several types of salt solutions in liquid sulfur dioxide. All cases show the polarization which is indicative of anodic passivation. Also it should be stated that all electrolytes are very dry for at no time are any of the solutions exposed to the atmosphere. All salts are dried before use and the cell is assembled in a dry box.

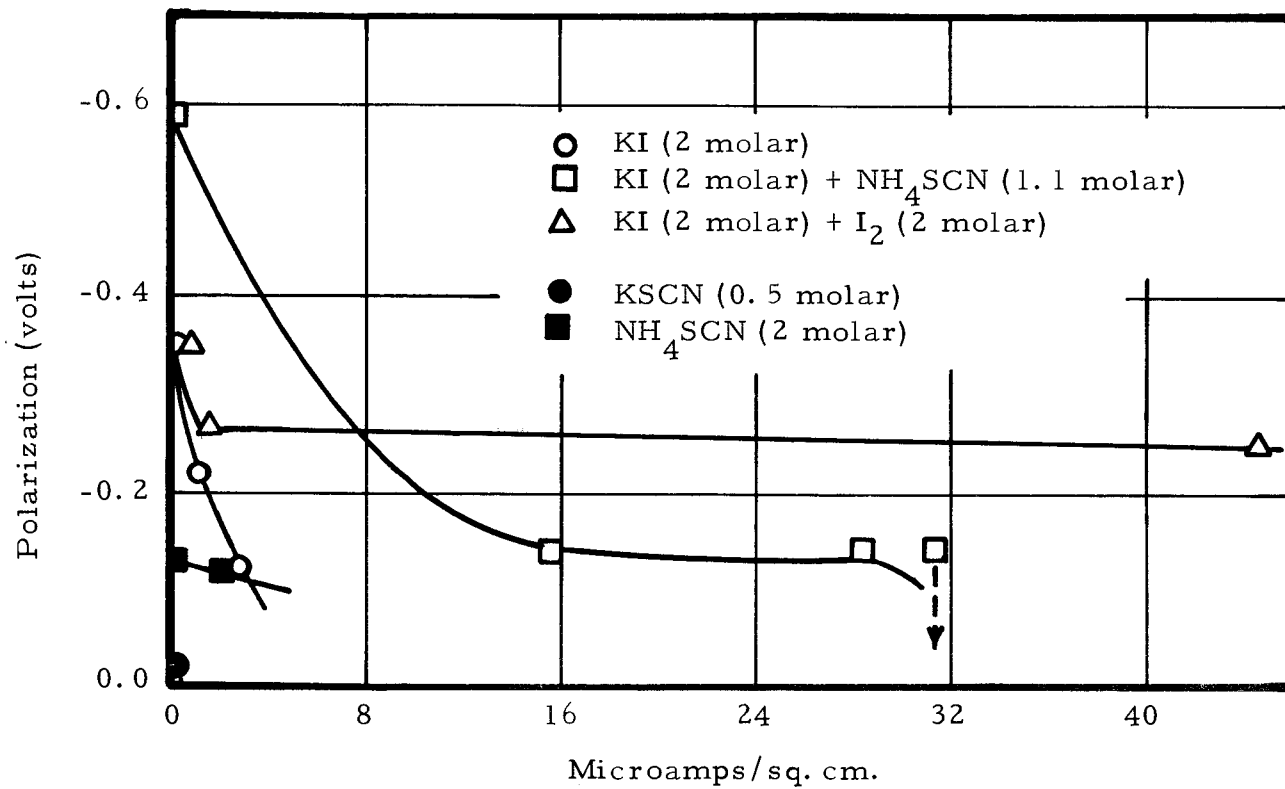
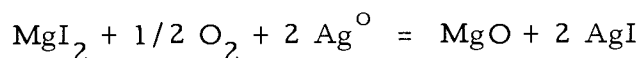


Figure 13. Magnesium anode polarization.

In an effort to determine the effects of other materials, compounds are added to the original electrolytes. In these additions the electrolyte is exposed to the atmosphere and some water can be absorbed. The compounds which are added are dried previously in order to eliminate the water contamination as much as possible. Figures 14, 15, 16, 17, and 18 show the results for various additives. It must be realized that the reference electrode is subject to some error because the concentration of the iodide ions is not controlled.

The results can be divided into two classes: electrolytes which are free of water and electrolytes which have water added to them. In all cases the addition of water has the effect of increasing the open circuit voltage and decreasing the polarization on current drain. The open circuit voltage of the cells which contain water varies between -0.84 volts and -1.42 volts (vs. Ag/AgI). Since the open circuit voltage is caused by an electrode couple, one concludes that the water reacts with either the magnesium metal or the anodic film and forms a new electrode couple. The potential for a typical reaction such as



is +0.747 volts at -20° C if the MgI_2 is dissolved in water (note: data not available for liquid sulfur dioxide). On the other

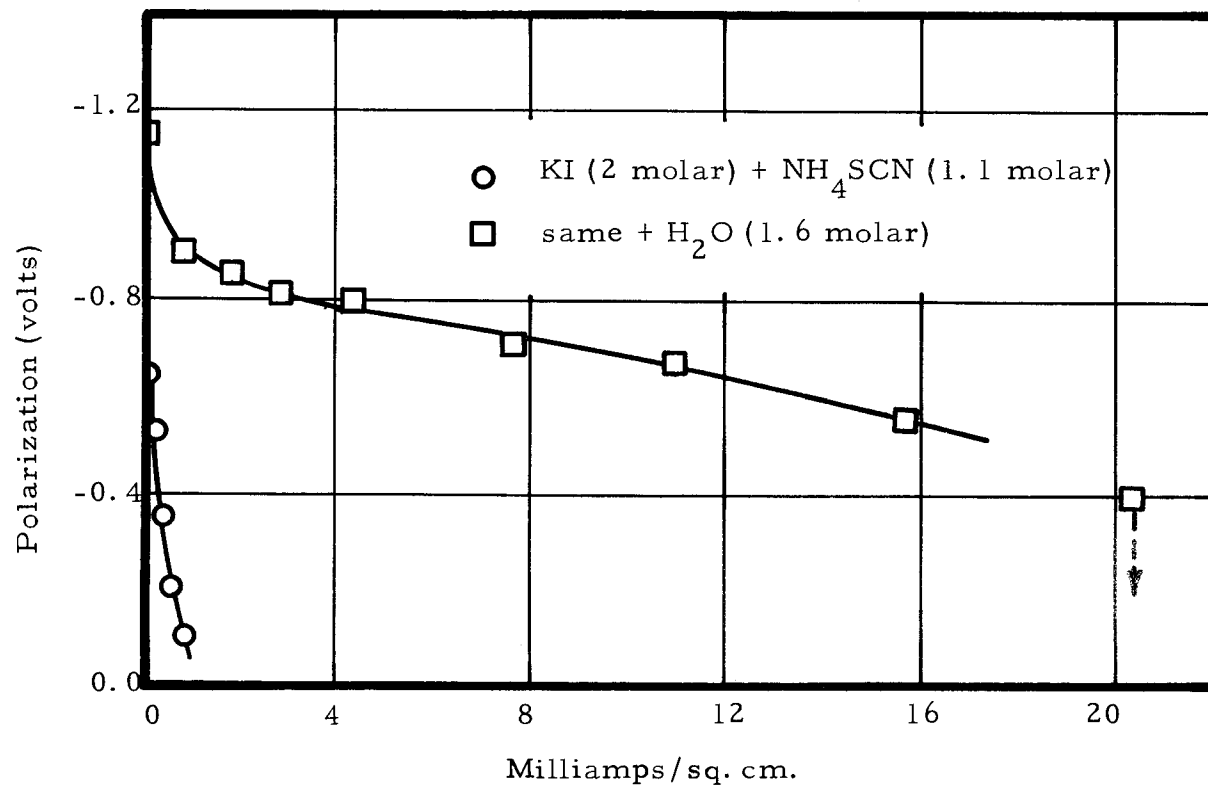


Figure 14. Magnesium anode polarization.

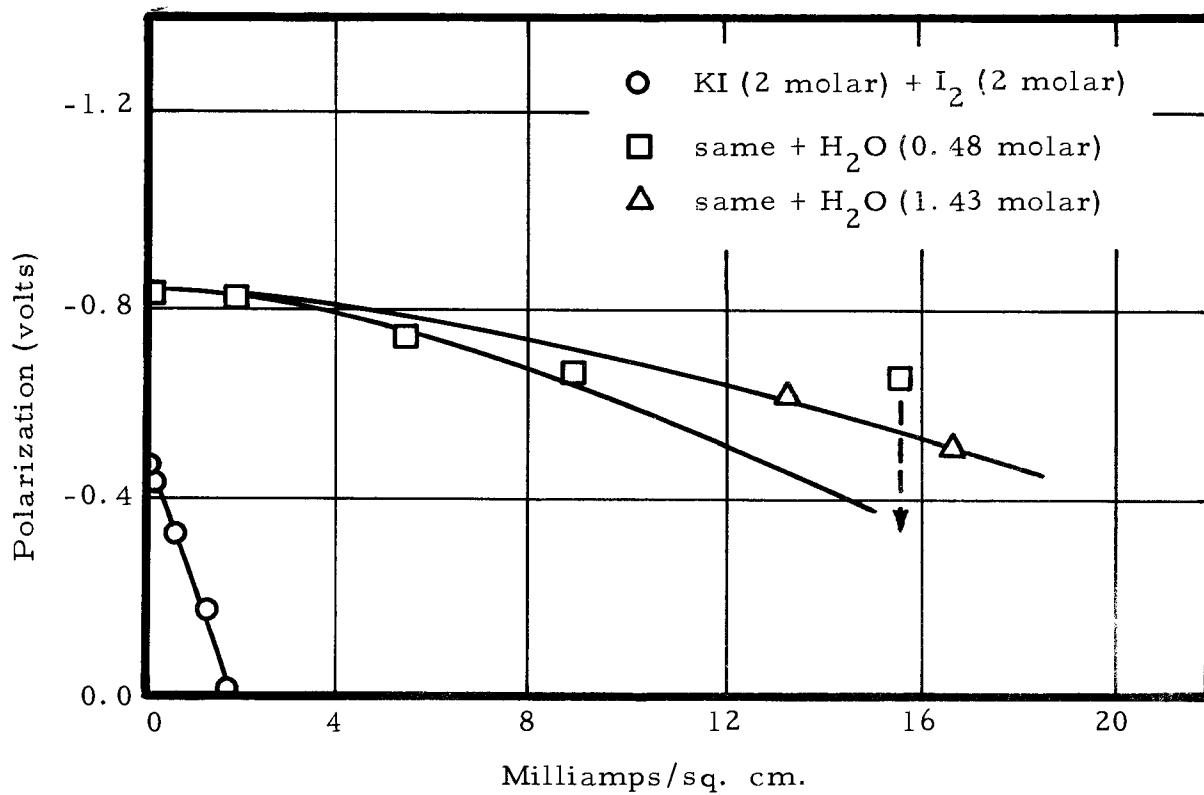


Figure 15. Magnesium anode polarization.

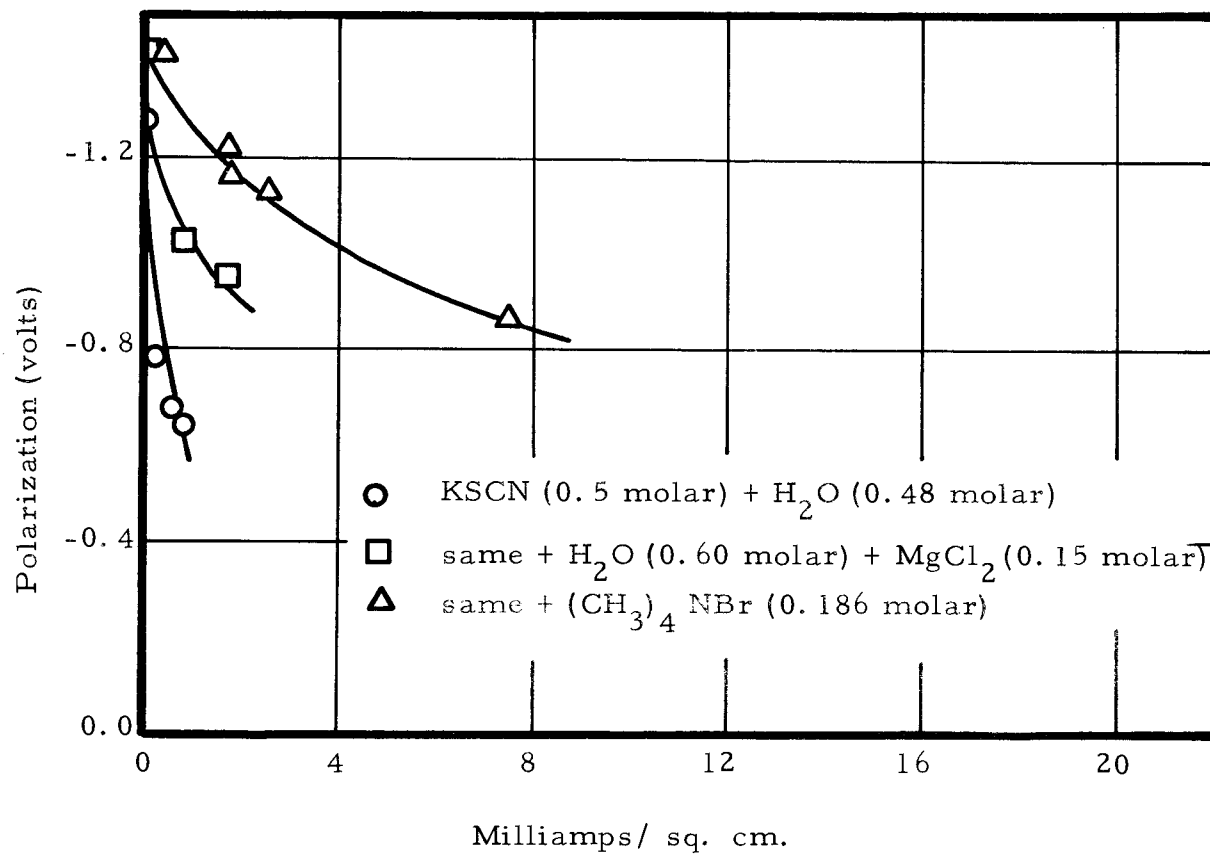


Figure 16. Magnesium anode polarization.

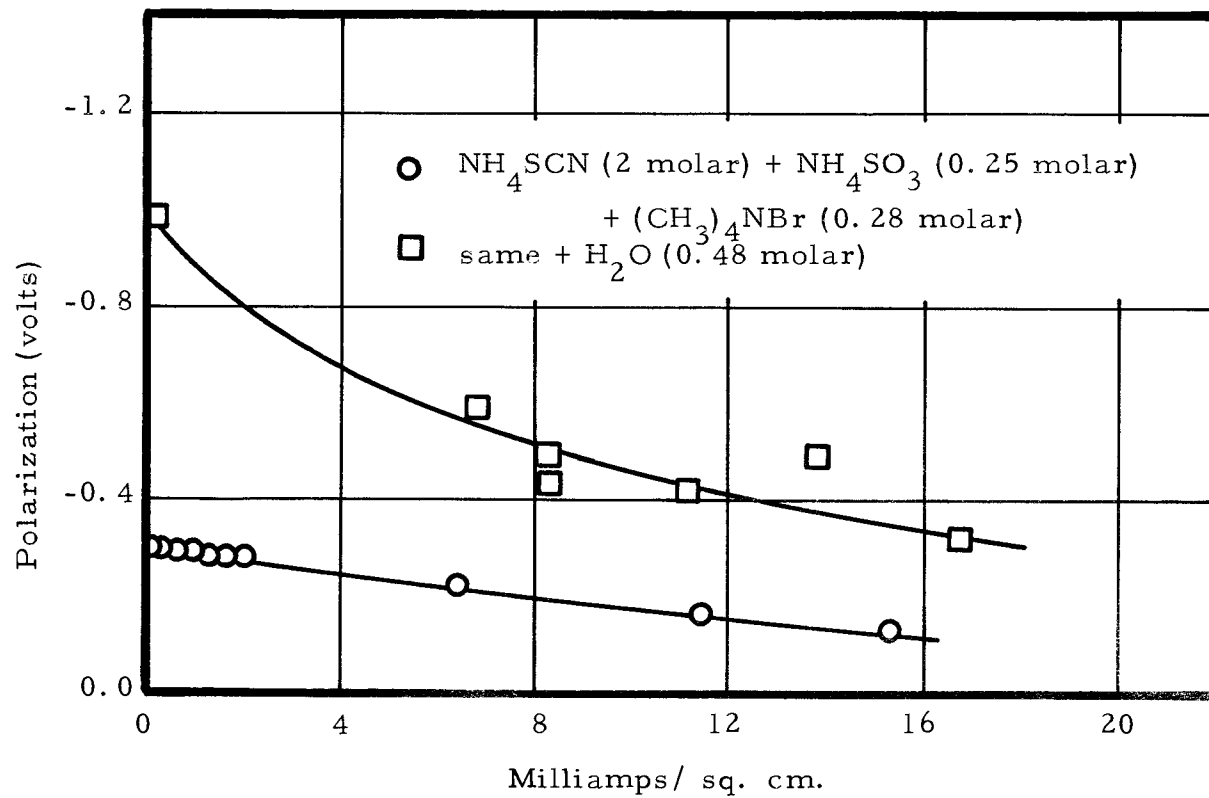


Figure 17. Magnesium anode polarization.

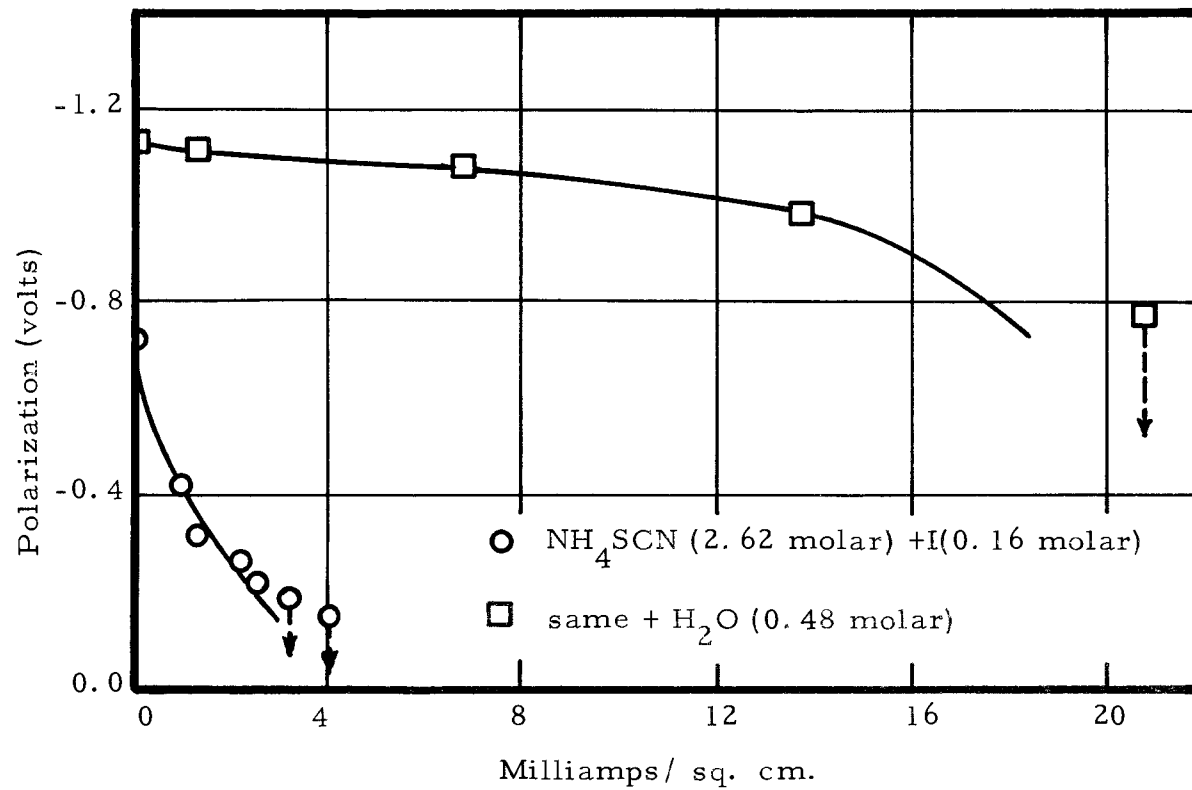
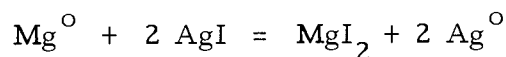


Figure 18. Magnesium anode polarization.

hand the potential of the reaction



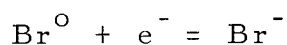
is +2.22 volts at -20° C if MgI_2 is dissolved in water. Therefore the actual potential determining reaction cannot be the second reaction, since the potential is much too high, or the first reaction, since the potential is too low. Hence the potential is caused by a combination of reactions involving the compounds contained in the anodic film.

The addition of tetramethyl ammonium bromide has the effect of decreasing the polarization. This is particularly noticeable in Figure 16 where it is added to an electrolyte containing water. It is known that tetramethyl ammonium compounds are quite soluble and also have a high equivalent conductivity in liquid sulfur dioxide (greater than 30 sq. cm./eq. ohm at a concentration greater than 2 molar). The increased ion concentration can lower ohmic polarization somewhat. Also, the bromide ions can decrease polarization, since the solubility of magnesium bromide is greater than the solubility of magnesium iodide. This increased solubility will allow higher current densities before the formation of the insulating film of crystals.

Figure 18 shows the results of an electrolyte solution exactly like cell #53 from the work of Schaschl (16). He obtained an open circuit voltage of -0.75 volts and a short circuit current of 8 ma. /sq. cm. Our results indicate an open circuit voltage of -0.73 volts (vs. Ag/AgI) (Note: Schaschl did not use a reference electrode and hence the open circuit voltages are not strictly comparable). Our current density is somewhat less indicating that Schaschl's cell could have contained some water since our results indicate that higher voltages and current densities occur when water is added.

Kinetic Parameters of the Bromine-Bromide Cathode Reaction

The cathode reaction in the liquid sulfur dioxide battery is probably



Since the rate of this reaction is very fast, one must study it with a method which eliminates many of the side effects which tend to obscure the activation polarization. One such method is the previously discussed double pulse method. By applying this method to various concentrations of bromine one can experimentally obtain the rate constant (k_s), the exchange current density (i_o), the transfer

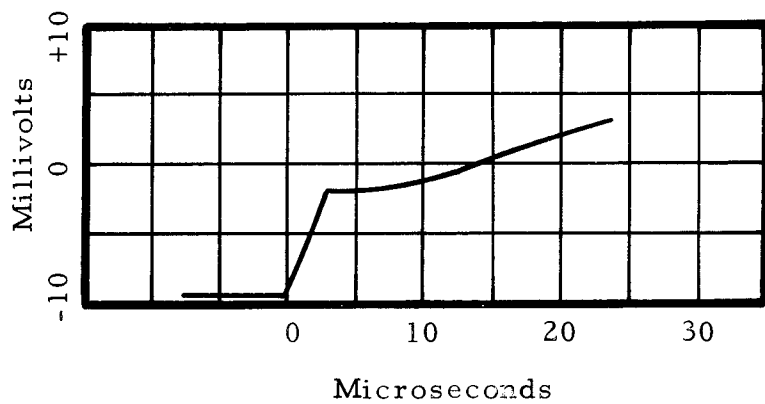
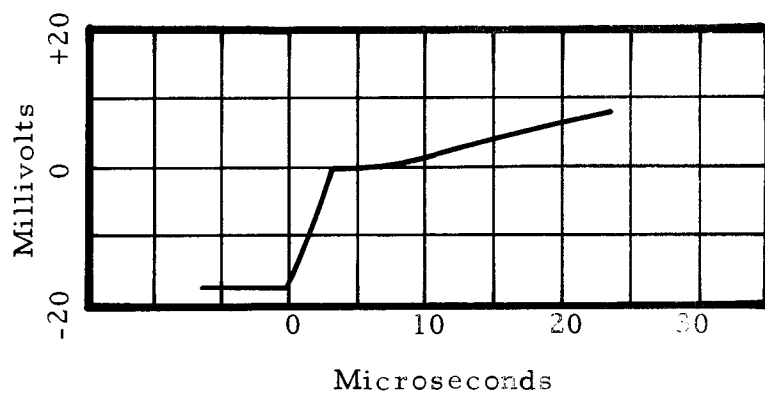
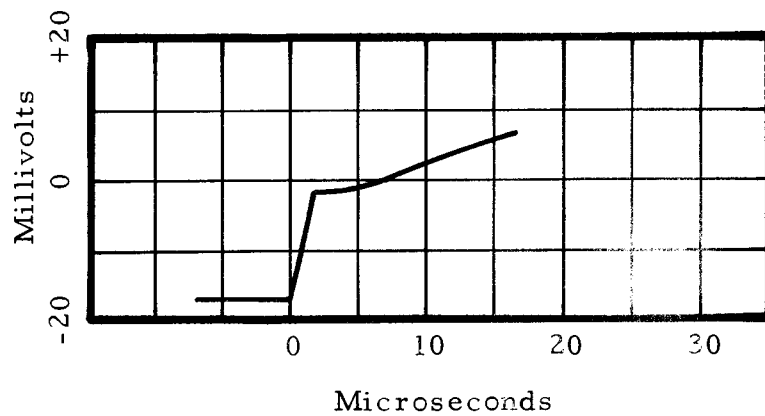
coefficient (α), and, sometimes, the diffusion coefficient (D).

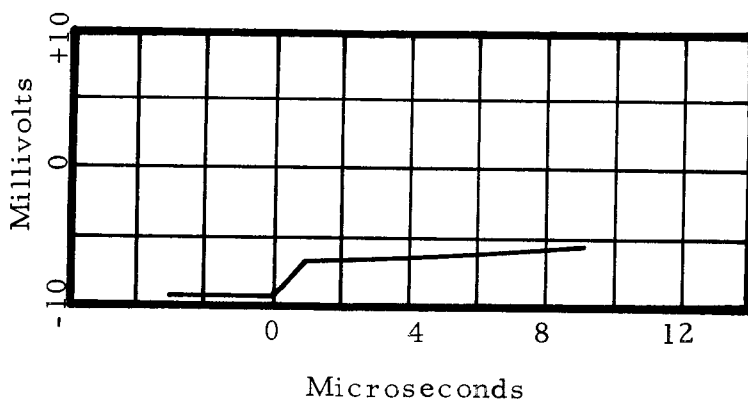
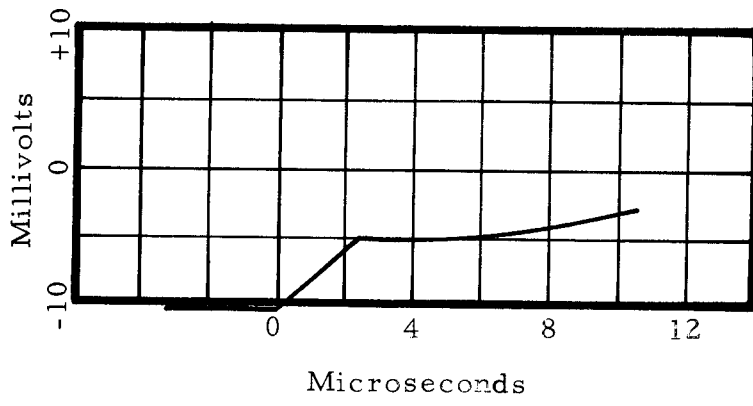
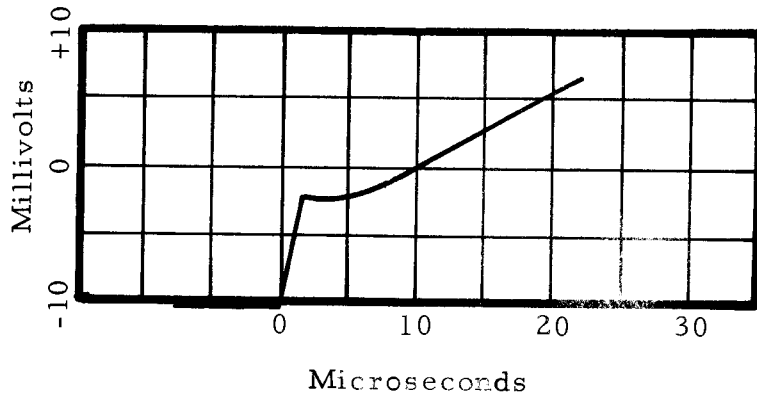
The apparatus and procedure are described in the section on zinc anode polarization. In this case a plane platinum indicator electrode is used, and the bromine is added through a small micropipette.

The six experimental traces are reproduced in traces #5 through #10. The apparent activation polarizations at t_1 are then plotted vs. $t_1^{1/2}$ and extrapolated to zero (Figure 19) in order to obtain the true activation polarization, free from concentration effects. From these values and Equation 9 one obtains the exchange current density (i_o). In order to calculate the transfer coefficient (α), one uses Equation 8 together with a plot of $\log i_o$ vs. $\log C_{Br^o}$ (Figure 20). Once the transfer coefficient is known, one can then calculate the rate constant (k_s) from Equation 8. All of the data and results are given in Table II.

The results listed in Table II justify the use of the double pulse method, since the rate constant (k_s) of approximately 0.23 cm./sec. is considered too fast for any steady-state method. This rate constant indicates that in an actual battery the polarization of the cathode reaction will be completely diffusion controlled.

Further theoretical analysis of some experimental data has been undertaken by Delahay (15) where he shows that the lines drawn





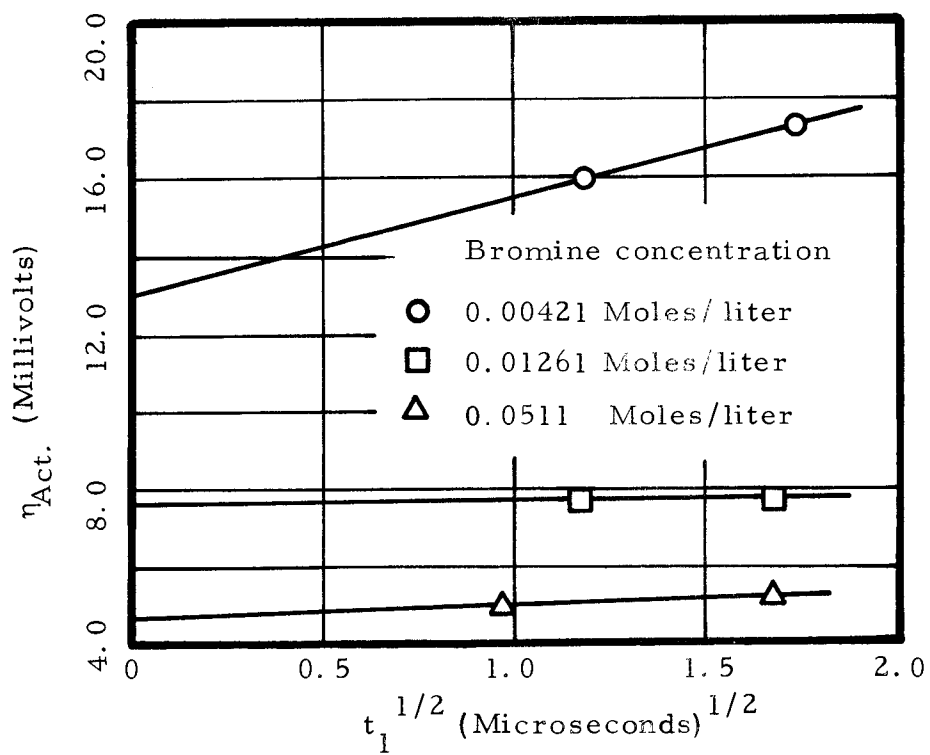


Figure 19. $\eta_{Act.}$ vs. $t_1^{1/2}$ for bromine reaction.

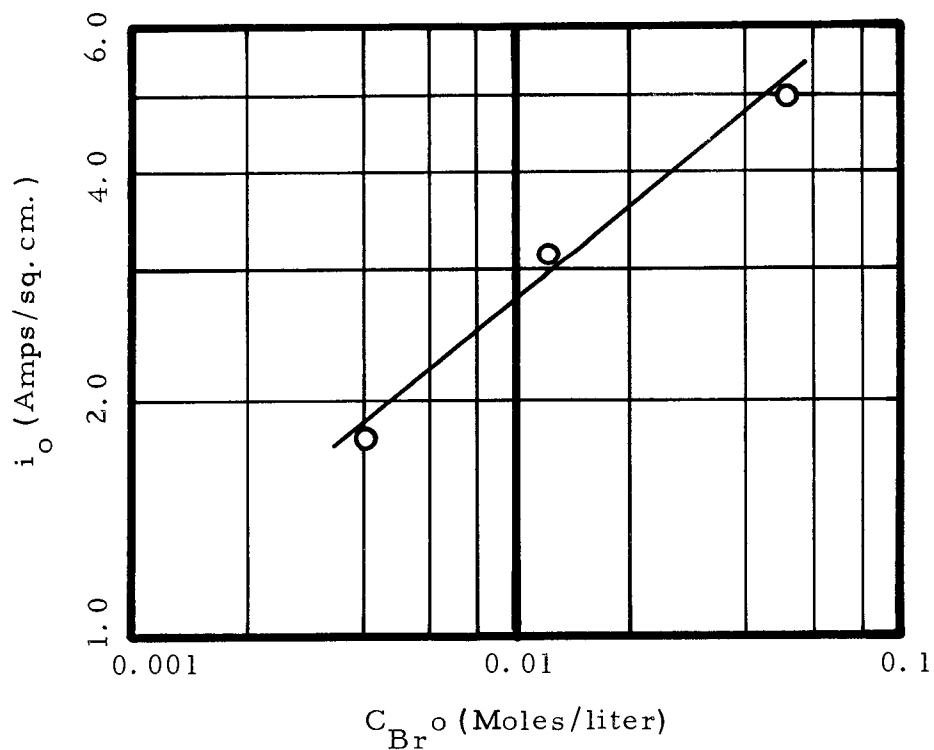


Figure 20. i_o vs. C_{Br^0} for bromine reaction.

TABLE II. RESULTS OF THE DOUBLE PULSE METHOD FOR BROMINE-BROMIDE REACTION.

#	KBr conc.	Br ^o conc.	Current*	t ₁	η _{Act.}	$\frac{t_1 \rightarrow 0}{\eta_{Act.}}$	i _o	k _s	Slope**
	moles —— liter	millimoles —— liter	ma	microsec.	mv	mv	amps —— sq. cm.	cm. —— sec.	mv —— microsec. ^{1/2}
5	0.647	4.21	0.555	1.4	16.05				
6	0.647	4.21	0.555	3.0	17.40	13.03	1.83	0.231	2.95
7	0.647	12.61	0.555	2.8	7.80				
8	0.647	12.61	0.555	1.4	7.75	7.59	3.14	0.254	-
9	0.647	51.1	0.555	2.4	5.35				
10	0.647	51.1	0.347	0.95	5.11	4.73	5.05	0.231	0.41

*Area of the indicator electrode is 0.000506 sq. cm.

**Figure 19

Note: Experimental value of the transfer coefficient (α) is 0.589.

in Figure 19 should follow the equation

$$\eta = \frac{RT i_o}{n^2 i} \left[1 + \frac{4}{3\pi^{1/2}} \frac{i}{n^2} \left(\frac{1}{D_{Br^o}^{1/2} C_{Br^o}} + \frac{1}{D_{Br^-}^{1/2} C_{Br^-}} \right) t_1^{1/2} + \text{smaller terms} \right] \quad (11)$$

for small values of t_1 . One can obtain the experimental slope in Figure 19 and then calculate an apparent experiment diffusion coefficient. Since the concentration of bromide ions is much greater than the concentration of the bromine molecules, one can neglect the $1/D_{Br^-}^{1/2} C_{Br^-}$ term in Equation 11. For a bromine concentration of 0.0511 moles/liter, we obtain an apparent diffusion coefficient of 12.8×10^{-5} sq. cm./sec., and for a bromine concentration of 0.00421 moles/liter we obtain an apparent diffusion coefficient of 22.2×10^{-5} sq. cm./sec.

For a bromine concentration of 0.01261 moles/liter the diffusion coefficient is extremely large. This can be explained by experimental errors such as incorrect compensation of the IR loss in the electrolyte for traces #7 and #8 and failure to accurately adjust the current of the second pulse in order to obtain a horizontal polarization (with time) in trace #8. These errors resulted in a low value of the slope in Figure 19 which leads to the high value of the diffusion coefficient.

The IR error also results in a high exchange current density which can be observed in Figure 20.

The true diffusion coefficient of bromine in liquid sulfur dioxide has not been measured but the diffusion coefficient of bromine in water at 12° C is 0.926×10^{-5} sq. cm./sec. (12). In order to obtain an estimate of the diffusion coefficient of bromine in liquid sulfur dioxide, we use the Einstein-Stokes relationship which is

$$(D\mu/T)_{\text{H}_2\text{O}} = (D\mu/T)_{\text{SO}_2} \quad (12)$$

The viscosity of water at 12° C is 1.236 centipoise and the viscosity of liquid sulfur dioxide at -20° C is 0.468 centipoise (17). Substituting these values into Equation 12 we obtain a value of 2.17×10^{-5} sq. cm./sec. for the diffusion coefficient of bromine in liquid sulfur dioxide at -20° C. Thus we see that the coefficient obtained from the double pulse method is abnormally high. This high value can be explained in either of two ways: one, the experimental results are very inaccurate, or two, bromine is adsorbed on the platinum electrode surface. This adsorption causes a high diffusion coefficient because the bromine does not have to diffuse to the electrode.

The most significant aspect of the application of the double pulse method to the bromine electrode reaction is that it

shows the feasibility of such a method in a practical battery electrode reaction. In past works, this method has been restricted to highly idealized systems (14, 15).

Other Cathode Materials

It has been found that the varieties of cathode materials are somewhat limited in liquid sulfur dioxide. This is mainly due to the solvent properties of liquid sulfur dioxide and the absence of hydrogen ions. Compounds such as meta-dinitrobenzene, ammonium nitrate, and lead dioxide were tried but gave no results. However, since a mixture of iodine and bromine give very good results, there is really no purpose in looking at cathode materials which are at more negative potentials, for these will have a lower open circuit voltage in a battery, and cathode materials which are more positive are few and far between.

Conductivity of IBr_3 * Solution

The specific conductivity of a 15% (weight) solution of IBr_3 in liquid sulfur dioxide at -20°C is $0.0017 \text{ (ohm cm.)}^{-1}$. This is a higher value than one would expect for a solution of two nonelectrolytes. It is supposed that the iodine and bromine associate in some manner to form ions but no attempt is made in the course of this

* IBr_3 is 3 moles of bromine plus 1 mole of iodine.

work to justify this belief.

Battery Cell Tests

Introduction

Many individual cell tests are conducted in an effort to determine some of the characteristics of a liquid sulfur dioxide battery. In order to have the tests as meaningful as possible, complete cells are tested in almost all cases, that is, cells which can deliver current on their own accord. It is important that complete cells be tested since the anode and cathode may have some interacting effects, and these effects can sometimes dictate battery feasibility. The cell apparatus and procedure are described in the apparatus section and in Figure 9.

In the following sections, the effect of anode materials, the effect of cathode materials, the effect of the type of electrolyte, the effect of current density, and the effect of temperature are examined. There are many more effects but we feel that those listed are the most valuable in the determination of the feasibility of a liquid sulfur dioxide battery.

Effect of Anode Materials

Anode materials in a $\text{KCl} \cdot \text{SbCl}_5$ (0.25 molar) + IBr_3 (15% wt) + SO_2 (l) electrolyte. Various anode materials are tested at a constant

current density of 20 ma./sq. cm. and ambient temperature. The discharge curves (CCV) are shown in Figure 21 along with the initial and final open circuit voltages (OCV).

Both the lithium-alloy anodes show markedly poorer discharge curves. An explanation of this phenomena could be the formation of a film of zinc or calcium salts at the anode surface. This phenomena is explained in detail in the previous section on zinc and magnesium polarization. The slightly lower initial OCV of the alloys compared to the pure lithium can be explained by the fact that the activity of lithium in the alloy is less than the activity of the pure lithium.

The potassium anode has the smallest polarization of all the anodes tested in this electrolyte. The high potential versus the Ag reference electrode is expected since potassium is one of the most negative materials in the standard redox tables. However, the potential of lithium in the standard redox tables is comparable to potassium, and because of this, we note that the initial OCV's of lithium and potassium are approximately equal. However we see in Figure 21 that the lithium polarizes to a greater extent than does potassium. This is probably due to the fact that potassium is kinetically more reactive than lithium.

We notice that sodium has a lower initial OCV as compared to the OCV of potassium or lithium. Once again, this is expected since sodium is not as negative as potassium or lithium in the standard

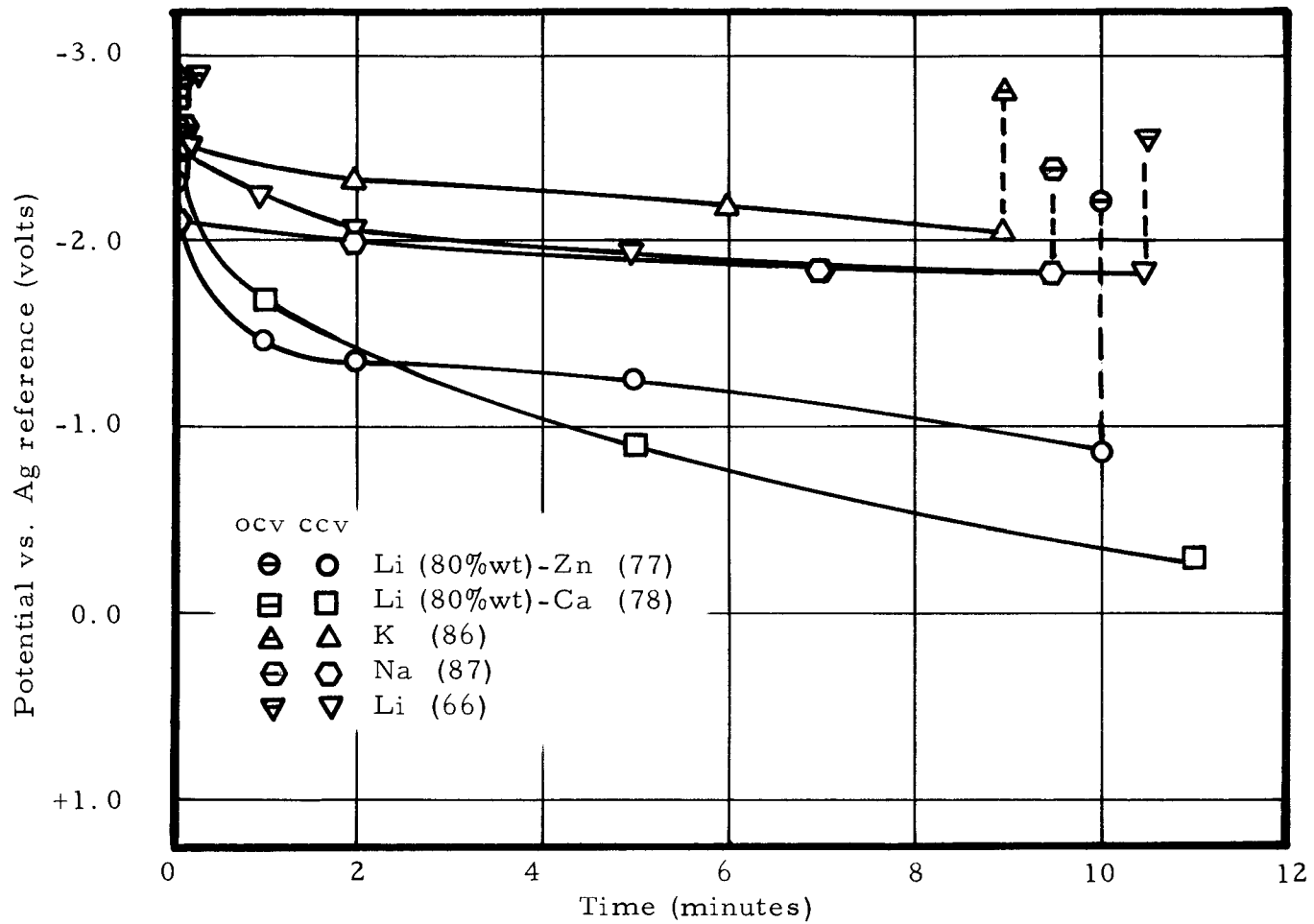


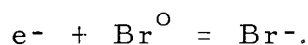
Figure 21. Effect of the anode material in the $\text{KCl} \cdot \text{SbCl}_5$ (0.25 molar) + IBr_3 (15%wt) + SO_2 (l) electrolyte at a current density of 20 ma./sq. cm. and at ambient temp.

redox tables. However sodium is kinetically more reactive than lithium. These two facts then combine to justify the similarity of the discharge curves for lithium and sodium after two minutes.

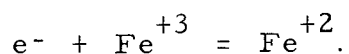
Anode material in a FeCl_3 (sat.) + KBr (sat.) + IBr_3 (15% wt) + SO_2 (l) electrolyte. Anodic behavior in this electrolyte is quite similar to the preceding electrolyte. The discharge curves are shown in Figure 22 for potassium, lithium, and calcium at ambient temperature and at a current density of 20 ma. /sq. cm. The explanation for the behavior of these curves is similar to the preceding case.

Effect of FeCl_3 and $(\text{CH}_3)_4\text{NBr}$ on the Cathode Reaction

It is postulated that the cathode reaction is



The addition of FeCl_3 to the electrolyte solution raises the question of an additional cathode reaction involving the reduction of the ferric ion to the ferrous ion or



In order to show the effect of FeCl_3 , four cells are studied. All four of the cells use an electrolyte of 85% SO_2 and 15% IBr_3 (by

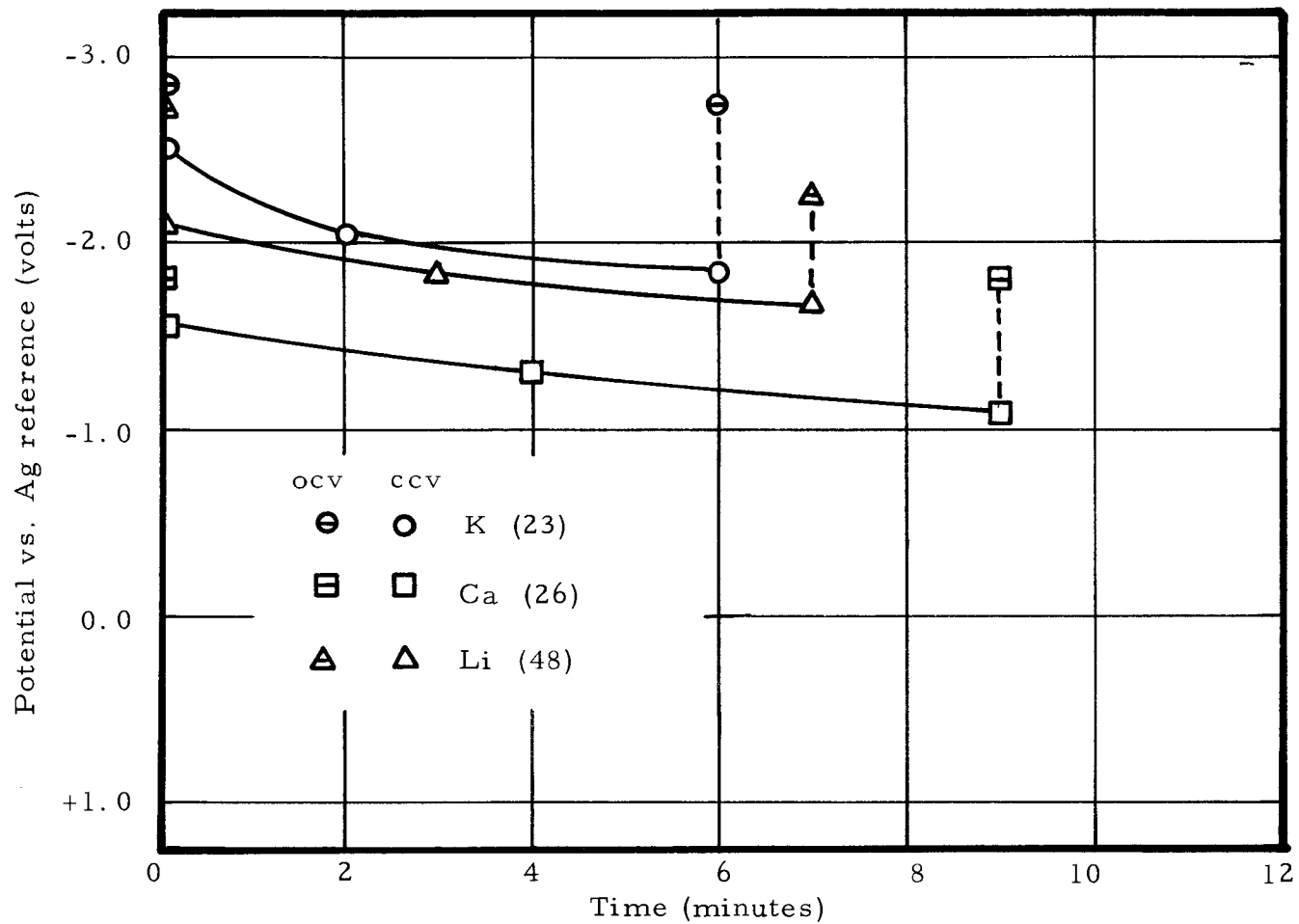


Figure 22. Effect of the anode material in the FeCl_3 (sat.) + KBr (sat.) + IBr_3 (15%wt) + SO_2 (1) electrolyte at a current density of 20 ma./sq. cm. and at ambient temperature.

weight) and a stainless steel anode surface. Cells #30 and #32 contain FeCl_3 crystals and cells #31 and #32 contain $(\text{CH}_3)_4\text{NBr}$ crystals. These crystals partially dissolve when the electrolyte is injected into the cell compartments and hence the electrolyte solution is considered saturated. All cells are maintained at ambient temperature during the run and a current density of 20 ma./sq. cm. is forced through them since there is no active anode.

The results of the cell runs are shown in Figure 23. The slight difference between cells #29 and #30 can be explained by the fact that the FeCl_3 increases the conductivity and thereby decreases the ohmic polarization of the electrolyte. However this difference can also be explained if one assumes that the FeCl_3 is reduced in the cathode reaction and thereby reduces the polarization at the cathode interface. In order to eliminate this effect, cells #31 and #32 contain $(\text{CH}_3)_4\text{NBr}$ to increase the conductivity to such a point that the increase in conductivity caused by the addition of FeCl_3 will be negligible. Of these two cells, the one which does not contain the FeCl_3 actually has slightly less polarization and this in fact is opposite to what will happen if the FeCl_3 is a factor in the cathode reaction. Therefore the effect of the FeCl_3 on the cathode reaction is very small or almost negligible. It must always be remembered that side reactions are also a factor which cannot be controlled and these reactions can be responsible for irreproducibility.

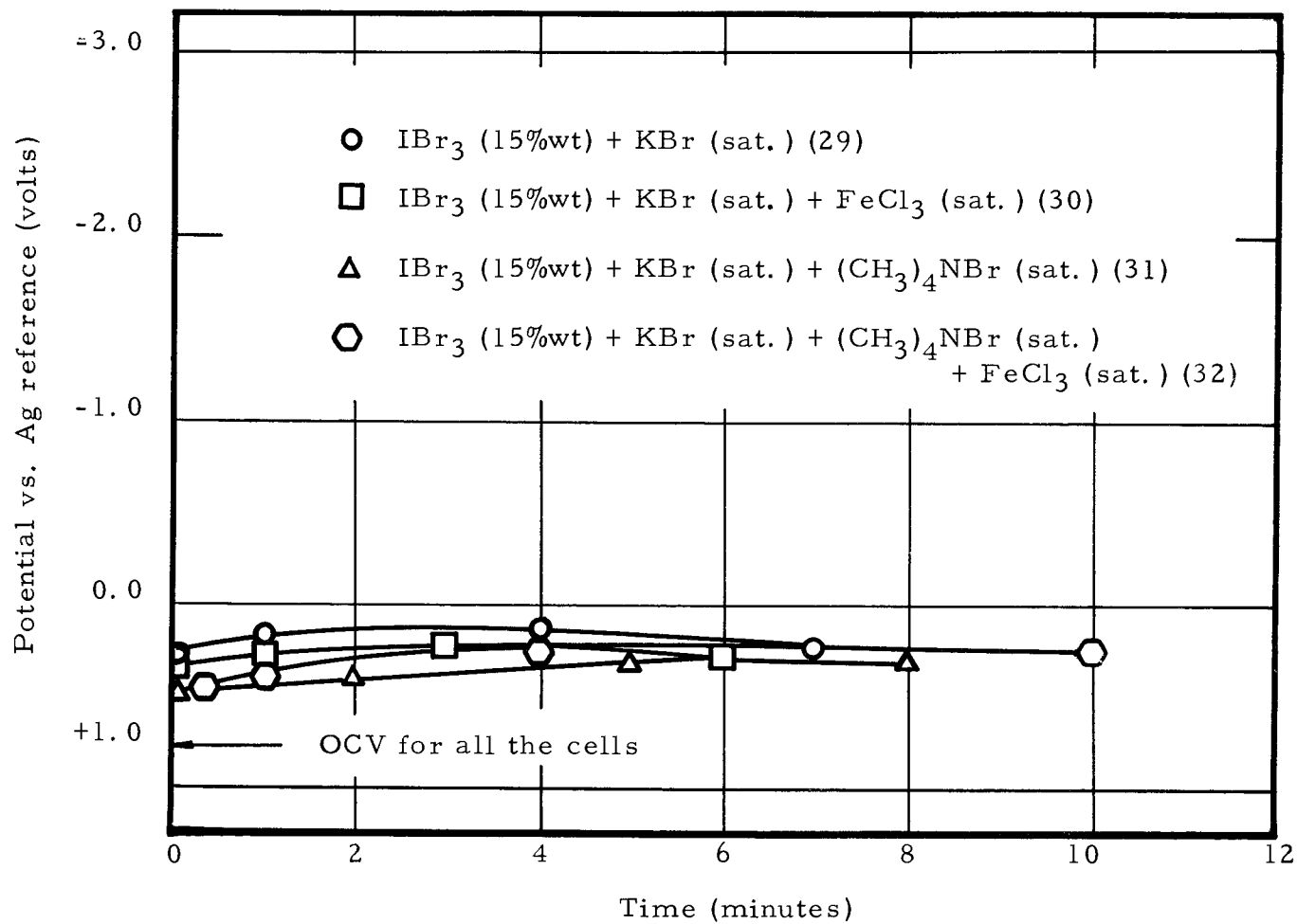


Figure 23. Effect of FeCl_3 and $(\text{CH}_3)_4\text{NBr}$ on the cathode reaction.

The addition of the $(\text{CH}_3)_4\text{NBr}$ has no effect on the cathode reaction. Its only effect on the cell is to increase the conductivity of the electrolyte.

Effect of the Reaction Surface on the Cathode Reaction

Three basic types of cathodes are evaluated. They are one, the stainless steel flat plane, two, the powdered carbon matrix, and three, the porous stainless steel disc. Of the three, only the carbon matrix (loosely packed powdered Shawinigan (Acetylene) Black) requires filter paper (Braun-Knecht-Heimann-Co. No. 28310) to hold it together and to separate it from the anode. Therefore in order to compare these, tests are included with the other two types of cathodes with and without a filter paper separator. Mechanically the cathode is separated from the anode by a Teflon spacer as shown in Figure 9. In all the tests, the anode is lithium, the electrolyte is $\text{KCl} \cdot \text{SbCl}_5$ (0.25 molar) + IBr_3 (15% wt) + SO_2 (1), the temperature is ambient and the current density is 20 ma./sq. cm.

Figure 24 illustrates that of the cathodes tested, the carbon matrix type provides the most efficient surface for the cathode reaction. The flat stainless plate gives the highest polarization as expected since its reaction area is the smallest of the three cathodes. In the case of the porous stainless disc and the flat stainless plane, the filter paper increases the polarization. This can be attributed

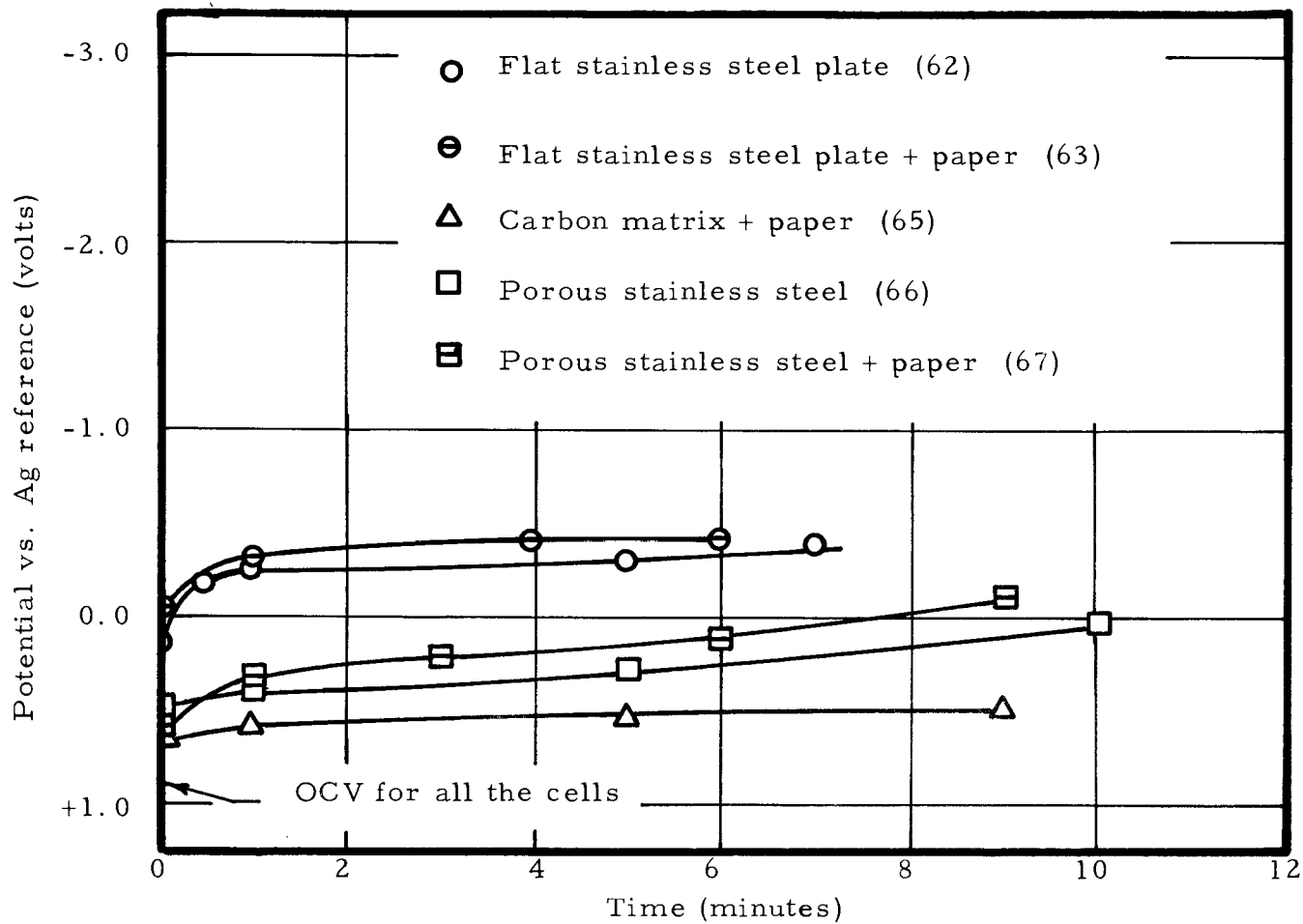


Figure 24. Effect of the reaction surface on the cathode reaction. The cell is Li/KCl·SbCl₅ (0.25 molar) + IBr₃ (15%wt) + SO₂ (l) /cathode at a current density of 20 ma./sq. cm. and at ambient temperature.

to the fact that the paper is a physical resistance to the diffusing cathode reactants and products. There is no doubt that the filter paper also increases the IR drop between the cathode and the reference electrode. The polarization of the cathode reaction could be further reduced if the carbon matrix would hold its form without the support of the filter paper.

Even though the carbon matrix gave the least polarization, we decided to use the porous stainless disc in all cell tests since it allows ease of construction. Therefore when evaluating the feasibility of a liquid sulfur dioxide cell from this work one should consider the added reduction in polarization which is possible if a carbon matrix cathode is used.

Effect of the electrolyte

Cathode. The three electrolytes $\text{KBr (sat.)} + \text{IBr}_3 (15\% \text{ wt})$, $\text{FeCl}_3 (\text{sat.}) + \text{KBr (sat.)} + \text{IBr}_3 (15\% \text{ wt})$, and $\text{KCl} \cdot \text{SbCl}_5 + \text{IBr}_3 (15\% \text{ wt})$ all have approximately the same effect on the cathode reaction. This is shown in Figure 23 and Figure 24. Therefore it is concluded that the cathode reaction involves only the IBr_3 .

Anode. The effect on anodic polarization by the three electrolytes previously listed is shown in Figure 25. The $\text{FeCl}_3 (\text{sat.}) + \dots$ and the $\text{KCl} \cdot \text{SbCl}_5 + \dots$ show similar discharge curves and open circuit potentials. However the cell which contains only the IBr_3

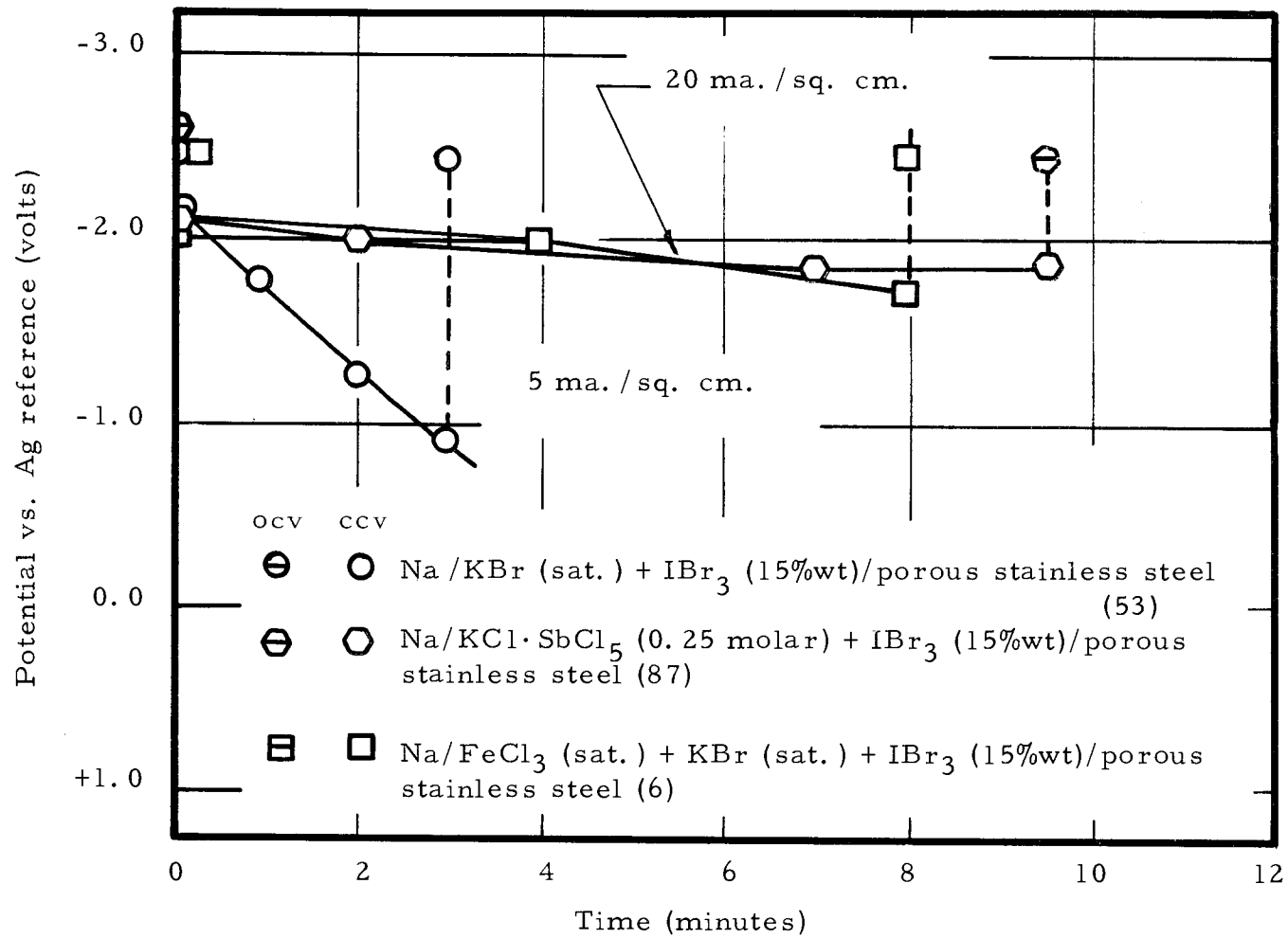


Figure 25. Effect of the electrolyte on the anode.

and KBr polarizes very rapidly. This polarization is very large even though the current density is only one fourth as large as the other two cells.

It appears that in order for an active anode to perform properly in a liquid sulfur dioxide electrolyte, the electrolyte must contain some compound capable of being reduced by the anode. In order that the anode be preserved during the life of the cell, this material must react only slowly with the active anode. The material must also be one which forms reaction products which are soluble in the sulfur dioxide solution. If such a substance is not present, the anode is coated with a film of reduction products formed from the solvent itself. These products, probably thiosulfites, etc., are insoluble and nonconductive, and hence cause large ohmic polarization as current flows through this film. This type of phenomena is present in all batteries in which one or both of the electrodes has a potential which is outside the decomposition potential of the solvent. In our case, if the reduction products of the solvent were soluble in the solvent, the addition of another compound would be unnecessary. Another explanation of the action of the FeCl_3 and SbCl_5 would be that these additives in some way form a complex with the electrochemical reaction products of the anode, and thereby improve the mass transfer of these products.

Current Density Effect

The effect of current density is shown in Figure 26. The four cells under study are Li/KCl·SbCl₅ (0.25 molar) + IBr₃ (15% wt) + SO₂ (1)/porous stainless steel at ambient temperature. These particular cells are chosen because they are relatively easy to construct since they utilize lithium anodes, and because they are representative in their discharge curves of all cells tested. Figure 26 shows the separate discharge or closed circuit voltage (CCV) as well as the initial and final open circuit voltages (OCV) for the anode and the cathode. The overall cell voltage is obtained by subtracting the cathode voltage from the anode voltage. For example, the initial OCV in all cases is 3.62 volts.

In all four of the cell tests, the initial OCV's are approximately the same, that is, within 100 millivolts of each other. Figure 26 indicates these voltages by an arrow for both the anode and the cathode.

As is expected, the polarization increases with current density. In the cases of current densities of 5 ma./sq. cm. and 20 ma./sq. cm., the lives of the cells are longer than 10 minutes. However, somewhere between current densities of 20 and 40 ma./sq. cm. the cells deteriorate quite rapidly, and in the case of a current density of 40 ma./sq. cm. the overall cell voltage becomes zero in 6.0 minutes.

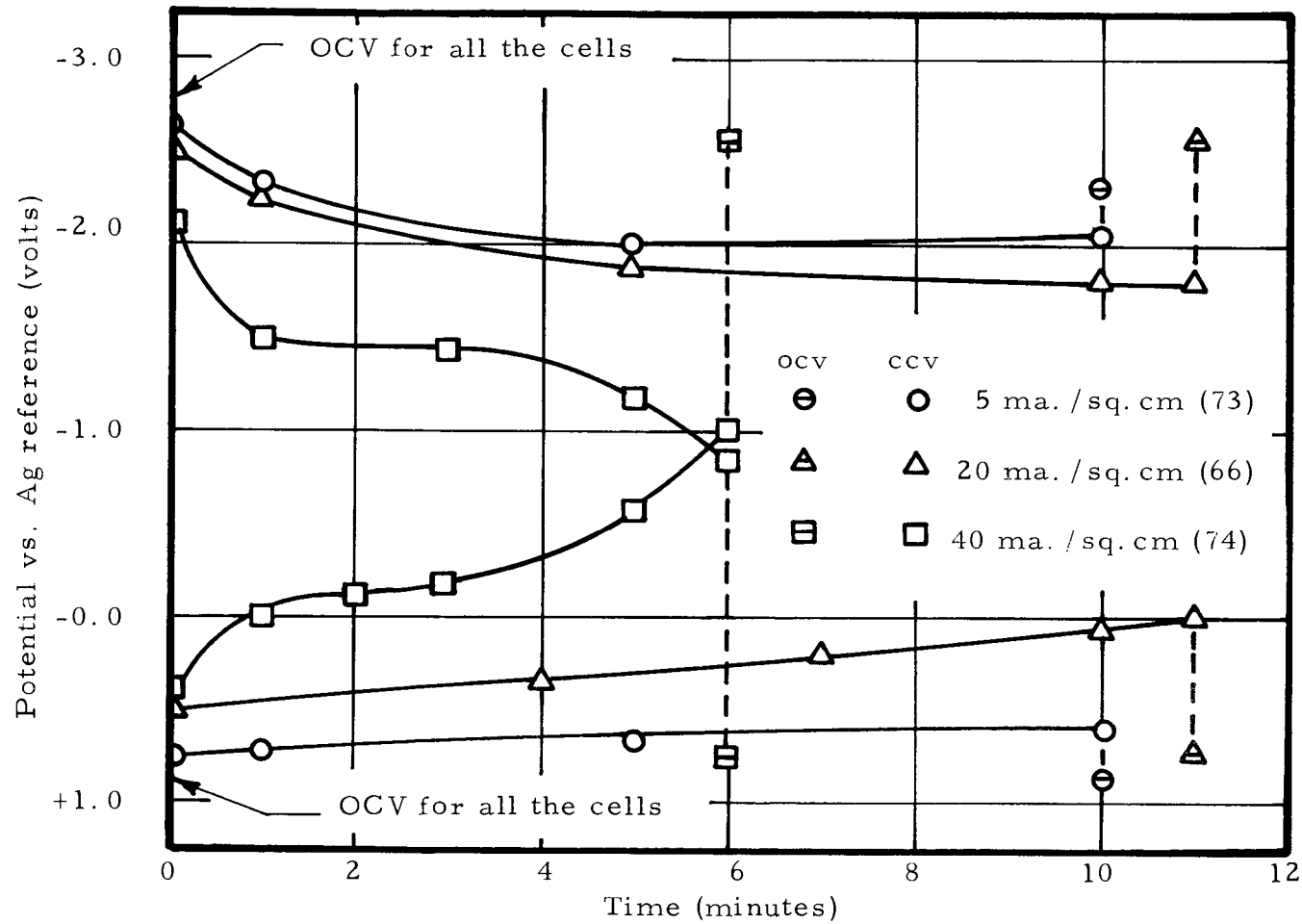


Figure 26. Current density on the cell $\text{Li}/\text{KCl}\cdot\text{SbCl}_5$ (0.25 molar) + IBr_3 (15%wt)/porous stainless steel at ambient temperature.

Since a constant current is forced through the cells, the life will appear to be much shorter than would be the case where a cell is discharged through a fixed resistance. This is because a cell discharging through a fixed resistance has a current density which continually decreases. This reduction in current increases the life of the cell. In fact, a cell discharging through a fixed resistance will never reach zero but will only approach it asymptotically.

Effect of Temperature

Cells are tested at the temperatures of ambient, 0°C , -22°C , and -44°C . All tests are conducted on the cell $\text{Li}/\text{KCl}\cdot\text{SbCl}_5$ (0.25 molar) + IBr_3 (15% wt) + SO_2 (l)/porous stainless steel at a current density of 20 ma./sq. cm. The results are shown in Figure 27.

Theoretically, the OCV should be approximately 4.00 volts for the reaction of lithium and bromine to form lithium bromide. The entropy change for this reaction is -20.4 cal./deg. C - g mole at 20°C and 1 atm in an aqueous media. Therefore the OCV should increase with a decrease in temperature. The results indicate an OCV of 3.70 volts at ambient temperature and 3.15 volts at -44°C . This result is opposite to that dictated by theory. However, since the lithium electrode is acting irreversibly, little value should be placed on this fact.

The results are too scattered to draw many analytical

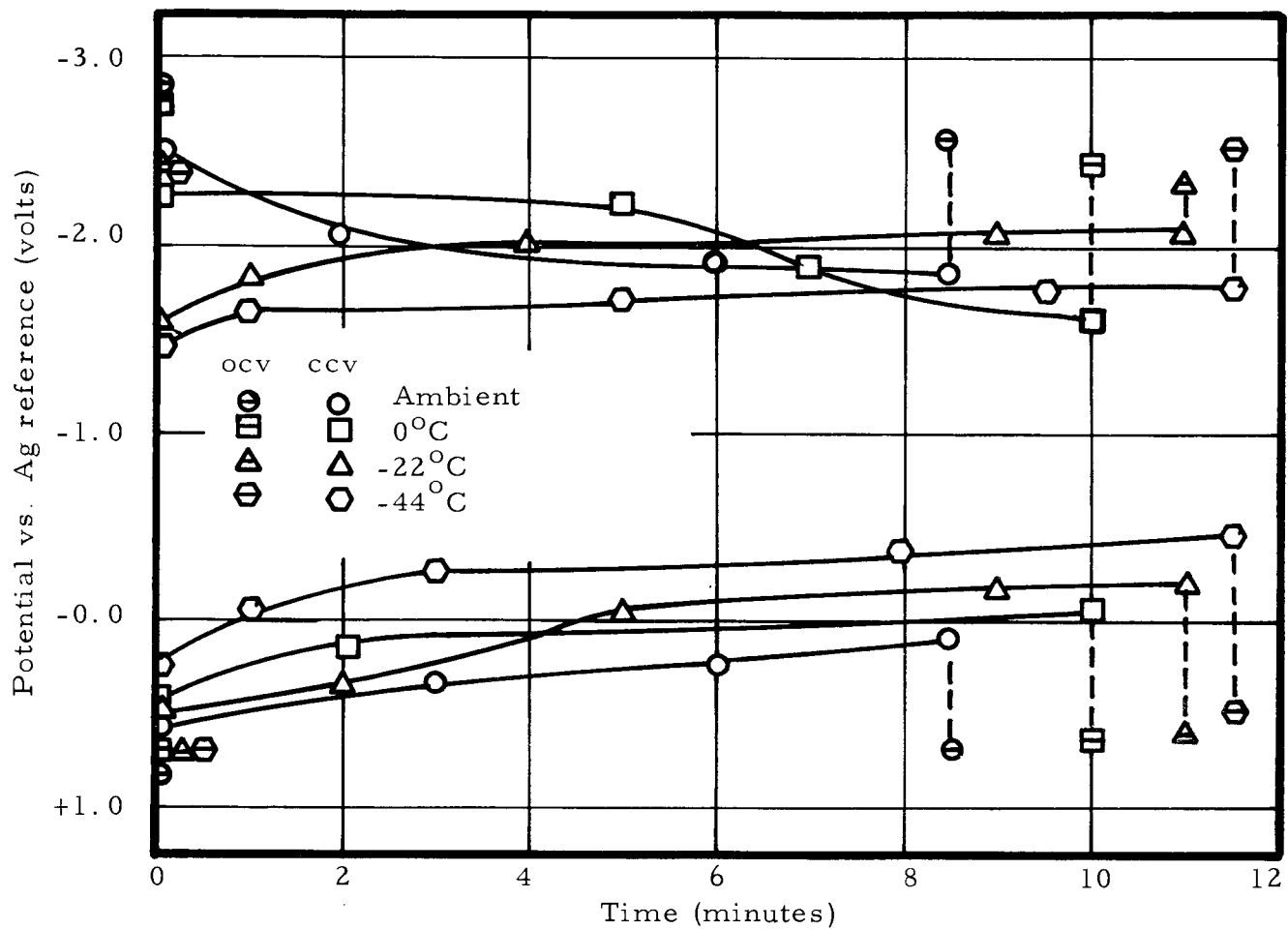


Figure 27. Effect of temperature on the cell $\text{Li}/\text{KCl} \cdot \text{SbCl}_5$ (0.25 molar) + IBr_3 (15%wt) + SO_2 (l)/porous stainless steel at 20 ma./sq. cm.

conclusions but one can say in general that a decrease in temperature results in lower overall cell voltage. This lower cell voltage is due to the anode reaction at short times and the cathode reaction at long times.

The decrease in anode polarization with time at the low temperatures could be explained by internal heating at the anode surface. It could also be explained by the slow removal of a film which may be initially present on the anode surface. The increase in cathode polarization with a decrease in temperature is probably due to the poor mass transfer of reactants and products to and from the porous stainless steel electrode.

Summary of Cell Tests

Some ninety individual cell tests were conducted. The results indicate that open circuit voltages greater than 3.70 volts and closed circuit voltages greater than 2.00 volts at 20 ma./sq. cm. can be obtained when utilizing alkali metals such as potassium or lithium as anodes and a mixture of iodine and bromine as a cathode.

It is believed that the only reason that alkali metals and halogens can exist in contact with one another is that a protective film is built up on the alkali metal surface. This film, while protecting the anode, also has a detrimental effect in that it causes ohmic polarization during passage of current through the cell. It is believed

that oxidizing agents such as FeCl_3 and SbCl_5 attack the anode and form soluble products. In other words, they tend to remove the protective film and hence make the surface much more conducive to the electrochemical reaction.

The cell tests show that sulfur dioxide cells can operate at all temperatures between room temperature and -44°C . Tests were not conducted at higher temperatures because of the safety hazard involved with high pressures. However there is no reason not to believe that sulfur dioxide cells will perform at these higher temperatures and pressures.

It should be pointed out that the electrolyte injection system should be changed for any future work. In many cell tests the electrolyte failed to penetrate properly. Of equal importance is the absolute necessity of making sure that the anode backing plate is never exposed to the electrolyte since the active anode and the metal backing plate will form a local corrosion cell. This cell causes rapid polarization of the anode and hence complete failure of the cell.

Mathematical Comparisons

The mathematical model states that the total polarization of an electrode includes resistive, activation, concentration, and

capacitive discharge polarization. Of these, the capacitive discharge is the only one not present after a short period of time.

Activation polarization of the cathode is calculated from Equation 7. As shown in the theoretical section, an exchange current density greater than 100 ma./sq. cm. yields an activation polarization of 0.1 volts at the extremely large current density of 10 amps/sq. cm. From Table II we see that the bromine reaction has an exchange current density of 5.05 amps/sq. cm. at a concentration of 51 millimoles/liter of bromine. Since the actual battery cell has a much higher concentration of bromine, it will have an even larger exchange current density. Therefore the activation polarization at the cathode is extremely small and would not appear in our polarization measurements. The same situation applies to the anode if we assume that the exchange current density of zinc and lithium are of the same order of magnitude. From Table I we see that the exchange current density of zinc is approximately 150 ma./sq. cm. Hence the activation polarization again will be so small that it will not appear in our measurements.

Concentration polarization is calculated from Equation 5 and is plotted in Figure 28. In order to calculate the concentration polarization, we must have the diffusion coefficients for bromine molecules and bromide ions. The diffusion coefficients are obtained by adjusting the actual diffusion coefficients of these molecules in water to

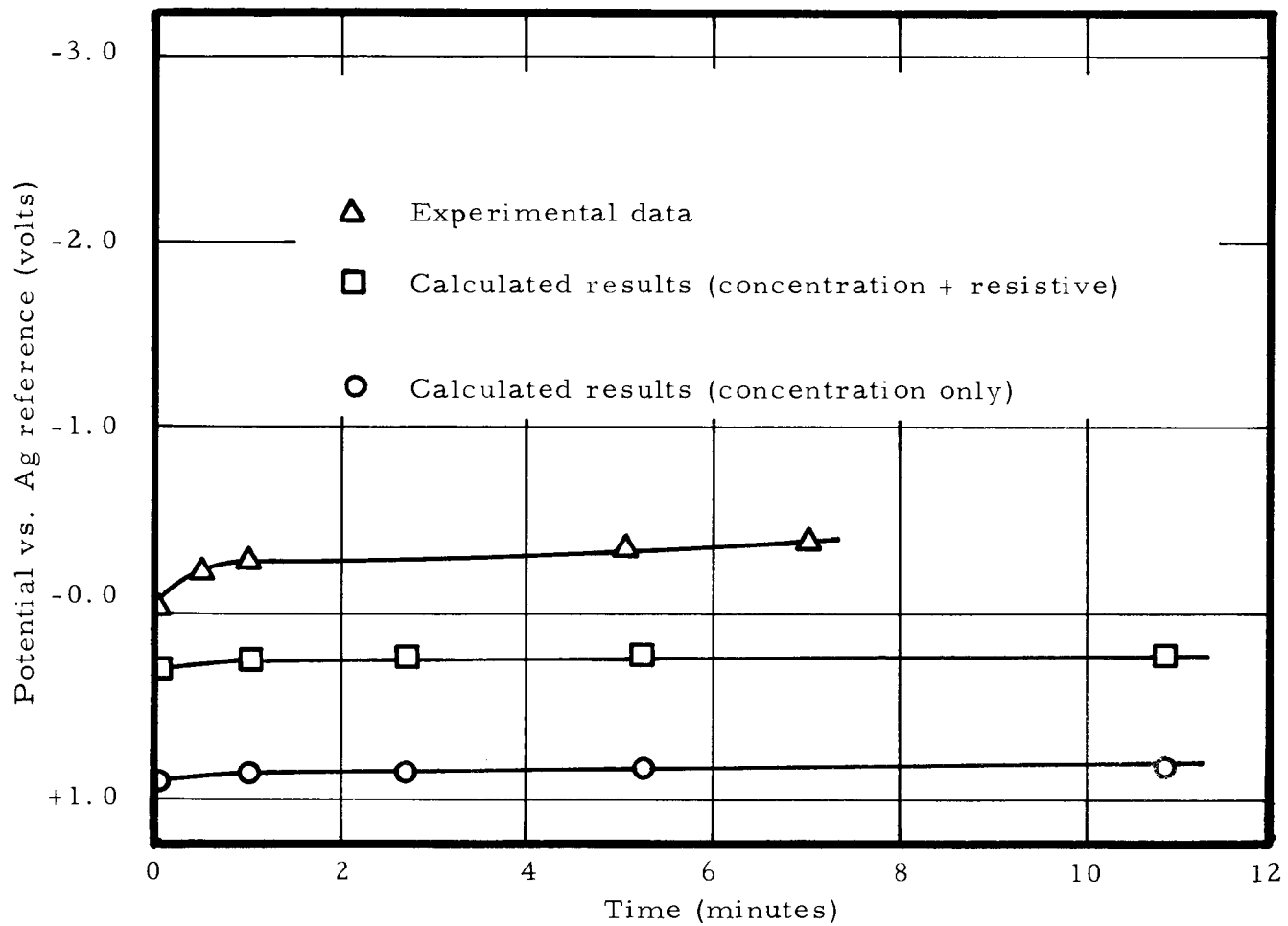


Figure 28. Mathematical comparison of the cell $\text{Li}/\text{KCl} \cdot \text{SbCl}_5$ (0.25 molar) + IBr_3 (15%wt)/Flat stainless steel plate at a current density of 20 ma./sq. cm. and at ambient temperature.

liquid sulfur dioxide by the Einstein-Stokes equation (12). Bromide is assumed to be in the form of potassium bromide and the diffusion coefficient is doubled to account for the migration term. The initial concentration of potassium bromide is assumed to be 0.1 molar.* As in the case of the activation polarization, the concentration polarization is very small and can be neglected at our current densities. The concentration polarization at the anode is not calculated since the anodic reaction is not reversible and hence does not fit the mathematical model.

Resistive polarization is the ohmic loss in the electrolyte. In the case of the electrolyte $\text{KCl} \cdot \text{SbCl}_5$ (0.25 molar) + IBr_3 (15% wt) + SO_2 (1) we can estimate the conductivity by assuming that the conductivities of the materials are additive. The specific conductivity of $\text{KCl} \cdot \text{SbCl}_5$ (0.25 molar) at -12°C in liquid sulfur dioxide is $0.0148 \text{ (ohm cm)}^{-1}$ and the specific conductivity of IBr_3 (15% wt) at -20°C in liquid sulfur dioxide is $0.0017 \text{ (ohm cm)}^{-1}$. In order to transform these to 20°C , we assume Walden's rule and thus calculate a total conductivity of $0.0216 \text{ (ohm cm)}^{-1}$. In a typical cell with a separation of 0.15 cm. and an area of 1 sq. cm., the total resistance

*Actually we have no grounds for this assumption and if the concentration polarization was significant we would have experimentally set the initial bromide concentration.

is 6.95 ohms. Hence at a current density of 20 ma./sq. cm., the total IR loss will be 0.14 volts. In the experimental cell apparatus, it was noticed that a small amount of KCl did not always dissolve. Assuming the worst possible condition, which is that none of the KCl dissolved and that the pure SbCl_5 is a nonconductor, then only the IBr_3 contributes to the conductivity and the total conductivity will be $0.00235 \text{ (ohm cm)}^{-1}$. The total IR loss at a current density of 20 ma./sq. cm. will then be 1.28 volts. If we assume that the reference electrode is located at the midpoint between the anode and cathode, then we will have a resistive polarization of 0.64 volts. Figure 28 shows the results for the maximum IR loss plus the concentration polarization.

In summary, the mathematical model fails to explain all the polarization in a liquid sulfur dioxide battery cell. This is particularly apparent in Figure 28 where the experimental results indicate a much higher cathodic polarization than is predicted from Equation 1.

IV. CONCLUSION

Throughout this work it has been our purpose to investigate those aspects of the behavior of the battery cell which we consider to be of importance in evaluating the feasibility of a liquid sulfur dioxide battery. We have evaluated such parameters as the exchange current density of zinc and bromine and the conductivity of IBr_3 dissolved in sulfur dioxide. We have studied the anodic polarization of zinc and magnesium in a glass cell where visual observation was possible. We have tested battery cells under realistic conditions. Finally we have compared the experimental results to the mathematical relationships derived in the early part of this work.

The exchange current density of bromine is so large that there will be virtually no activation polarization at the cathode. If we assume that the exchange current density of zinc is of the same order of magnitude as the exchange current density of the alkali metal,* then we can safely say that there will be virtually no activation polarization at the anode.

The conductivity of the IBr_3 solution is not very large; therefore, IR losses in the electrolyte will become important

*It was originally planned to measure the exchange current density of the alkali metals, but since their potentials are more negative than the decomposition potential of sulfur dioxide, it was not considered theoretically possible.

at higher current densities. This IR loss can be decreased if other soluble conducting materials such as FeCl_3 and $\text{KCl} \cdot \text{SbCl}_5$ are added to the electrolyte.

The concentration polarization as mathematically derived (recall that only diffusion was assumed and no convection terms were included; therefore, the mathematical model will be the worst possible case of concentration polarization) is very small and can be neglected at current densities of about 20 ma./sq. cm. At higher current densities there may be a tendency for the cathode to reach limiting current. However, in this work this point was never reached.

We have shown that all of the polarizations which have been treated theoretically, except resistive polarization, are negligible. Therefore we must conclude that the polarization of the sulfur dioxide cells is caused by IR loss in the electrolyte and an insulating film on the anode and cathode surface. This conclusion was reached by extending the results obtained in the visual observations in the zinc and magnesium polarization experiments where an insulating film was observed. We further conclude that the primary effect of the FeCl_3 or $\text{KCl} \cdot \text{SbCl}_5$ in the case of the alkali metals, and water in the case of magnesium, is to remove the insulating film from the anode surface. We have also shown that these additives have no effect on the cathode process.

One must consider at this point the value of the mathematical

treatment in this work. In the case of the liquid sulfur dioxide cell, it served the purpose of indicating only that the theoretical effects were negligible. However, one cannot say in general that this will always be the case and hence we conclude that a mathematical treatment should always be considered. In the future, however, the mathematical formulation should include a term for the formation of insulating films on the electrode surfaces.

A secondary but important purpose of this work was to evaluate the double pulse method for the evaluation of the exchange current density of very fast reactions. We have shown that it is feasible in an anodic and cathodic reaction. In particular, the double pulse method is required in the bromine reaction since in any single pulse or steady state process, the activation polarization would be totally obscured by other polarization effects.

Finally, the overall purpose of this work was the determination of the feasibility of the high energy, short life liquid sulfur dioxide battery. We believe that such a battery is indeed feasible since activation polarization is negligible, concentration polarization is small, the theoretical capacity is 563 watt-hr. /lb (assuming Li and Br), the open circuit voltage is greater than 3.7 volts in some cases, and the closed circuit voltage is greater than 2.0 volts at a current density of 20 ma. /sq. cm for a period longer than six minutes. Figure 29 shows a liquid ammonia cell (courtesy of the

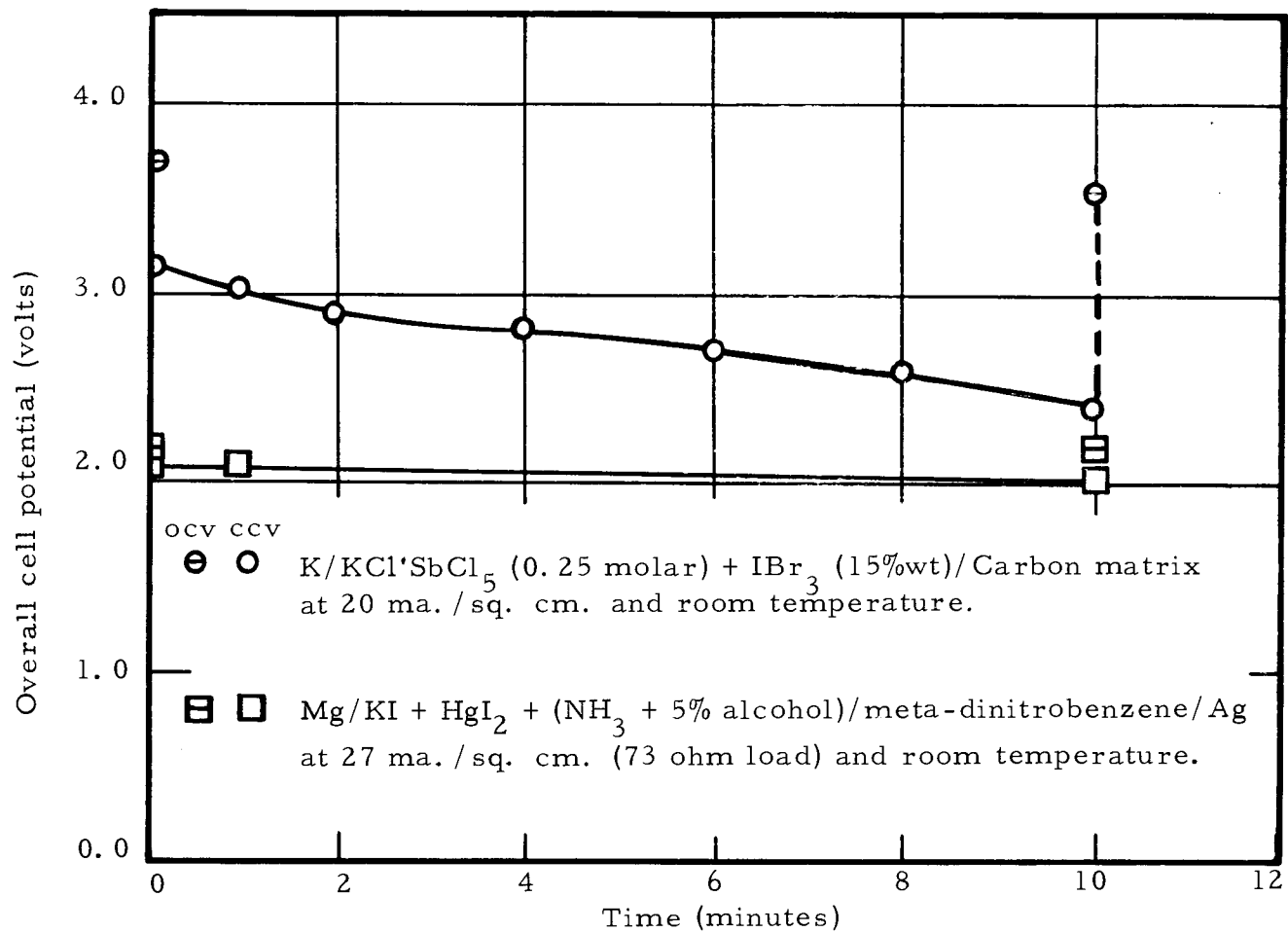


Figure 29. Comparison of a liquid sulfur dioxide cell and a liquid ammonia cell.

Naval Ordnance Laboratory, Corona, California) and a liquid sulfur dioxide cell. The liquid ammonia cell has been in development for several years while the sulfur dioxide cell has received very little attention. It should be pointed out that the liquid ammonia cell shown in Figure 29 is operating at a current density which is considered well below its maximum while the liquid sulfur dioxide cell is operating at a current density considerably closer to its maximum at this time. Also, the liquid ammonia battery has a much longer life. Nevertheless, we believe that with the proper development program, a liquid sulfur dioxide battery would become very competitive to such high energy batteries as the liquid ammonia battery described here.

BIBLIOGRAPHY

1. Audrieth, Ludwig F. and Jacob Kleinberg. Non-aqueous solvents. New York, Wiley, 1953. 284 p.
2. Bagster, L. S. and B. D. Steele. Electrolysis in liquified sulfur dioxide. Transactions, Faraday Society 8:51-67. 1912.
3. Berzins, Talivaldis and Paul Delahay. Kinetics of fast electrode reactions. Journal of the American Chemical Society 77:6448-6453. 1955.
4. Bruner, L. and E. Bekier. Uber die elektrische Leitfähigkeit und Elektrolyse von Brom, Jodbromid, Jodchlroid und Jodtrichlorid in flussigem SO_2 . Zeitschrift fur Physikalische Chemie 84:570-584. 1913.
5. Cady, Hamilton Perdins and Robert Taft. Electrolysis in liquid sulfur dioxide. Journal of Physical Chemistry 29:1075-1084. 1925.
6. Centnerszwer M. and J. Drucker. Electrolyse in flussigem Schwefeldioxyd. Zeitschrift fur Elektrochemie und Angewandte Physikalische Chemie 29:210-214. 1923.
7. Cruse, Kurt. EMK-Messungen in flussigem Schwefeldioxyd. Zeitschrift fur Elektrochemie und Angewandte Physikalische Chemie 46:571-590. 1940.
8. Elving, Philip J. and Joseph M. Markowitz. Chemistry of solutions in liquid sulfur dioxide. Journal of Chemical Education 37:75-81. 1960.
9. Elving, Philip J. and Joseph M. Markowitz. Voltammetry in liquid sulfur dioxide. II. Behavior of triphenylchloromethane. Reduction of the triphenylmethyl free radical. Journal of Physical Chemistry 65:686-690. 1961.
10. Elving, Philip J., Joseph M. Markowitz and Isadore Rosenthal. Voltammetry in liquid sulfur dioxide. I. Technique and theoretical problems. Journal of Physical Chemistry 65:680-686. 1961.

11. Hajek, M. Jan. Electrolyte pour electrodes de poids leger. French patent 1.000.044. October 8, 1949. 2 p.
12. Hodgeman, Charles D. (ed) Handbook of chemistry and physics. 37th ed. Cleveland, Chemical Rubber, 1956. 3156 p.
13. Konecny, J. A survey of the potential of sulfur dioxide reserve battery activation. Corona, California, U. S. Naval Ordnance Laboratory, January 16, 1958. 17 p. (NAVORD Report 4639 or NOLC Report 394).
14. Laitinen, H. A., R. P. Tischer and D. K. Roe, Exchange current measurements in KCl-LiCl eutectic melt. Journal of the Electrochemical Society 107:546-555. 1960.
15. Matsuda, Hiroaki, Syataro Oka and Paul Delahay. Analysis of the double pulse galvanostatic method for fast electrode reactions. Journal of the American Chemical Society 81:5077-5081. 1959.
16. Schaschl, Edward and Hugh J. McDonald. A low temperature liquid sulfur dioxide battery. Journal of the Electrochemical Society 94:299-308. 1948.
17. Steele, Bertram D. On the electrolysis of salt solutions in liquified sulfur dioxide at low temperatures. Chemical News 96:224-225. 1907.
18. Taniguchi, Harry and George J. Janz. Preparation and reproducibility of the thermal electrolytic silver-silver chloride electrode. Journal of the Electrochemical Society 104:123-127. 1957.